

**Evaluation Of Multisensory MEMS-based Accelerometers for Real-time Structural  
Dynamic Response**

A Thesis of

**Master of Science**

By

**Muhammad Yasir Gul**

(NUST-2019-MS SE 00000319496)



**July 2022**

Department of Structural Engineering

**Military College of Engineering, Risalpur**

**National University of Science & Technology**

**Islamabad, Pakistan**

**(2022)**

This is to certify that the

thesis titled

**Evaluation Of Multisensory MEMS-based Accelerometers for Real-time Structural Dynamic Response**

Submitted by

**Muhammad Yasir Gul**

(00000319496)

has been accepted towards the partial fulfillment

of the requirements for the degree of

Master of Science in Structural Engineering

---

**Dr. Muhammad Rizwan**

Associate Professor,

Department of Structural Engineering,

Military College of Engineering, Risalpur

National University of Sciences and Technology (NUST), Islamabad

## **THESIS ACCEPTANCE CERTIFICATE**

Certified that the final copy of MS thesis written by Muhammad Yasir Gul, (Registration No. NUST-2019-MS SE-00000319496), of MILITARY COLLEGE OF ENGINEERING (MCE), Risalpur has been vetted by the undersigned, found complete in all respects as per NUST Statutes/Regulations, is free of plagiarism, errors, and mistakes and is accepted as partial fulfillment for the award of MS degree. It is further certified that necessary amendments as pointed out by GEC members of the scholar have also been incorporated in the said thesis.

Supervisor: \_\_\_\_\_

**Associate Professor** (Dr. Muhammad Rizwan)

## **DECLARATION**

I certify that this research work titled “**Evaluation of Multisensory MEMS-based Accelerometers for Real-time Structural Dynamic Response**” is my own work. The work has not been presented elsewhere for assessment. The material that has been used from other sources it has been properly acknowledged / referred.

---

Signature of Student

Muhammad Yasir Gul

(2019-NUST-MS SE-00000319496)

## PLAGIARISM CERTIFICATE

It is certified that MS Thesis Titled “Evaluation Of Multisensory MEMS based Accelerometers for Real-time Structural Dynamic Response” by Muhammad Yasir Gul has been examined by us.

We undertake the follows:

- Thesis has significant new work/knowledge as compared already published or are under consideration to be published elsewhere. No sentence, equation, diagram, table, paragraph, or section has been copied verbatim from previous work unless it is placed under quotation marks and duly referenced.
- The work presented is original and own work of the author (i.e., there is no plagiarism) No ideas, processes, results, or words of others have been presented as Author own Work.
- There is no fabrication of data or results which have been compiled/ analyzed.
- There is no falsification by manipulating research materials, equipment, or processes, or changing or omitting data or results such that the research is not accurately represented in the research record.
- The thesis has been checked using TURNITIN (copy of originality report attached) and found within limits as per HEC plagiarism Policy and instructions issued from time to time.

Name & Signature of Student

Muhammad Yasir Gul

Signature: \_\_\_\_\_

Name & Signature of Supervisor

Dr. Muhammad Rizwan

Signature: \_\_\_\_\_

## **COPYRIGHT STATEMENT**

Copyright in text of this thesis rests with the student author. Copies (by any process) either in full, or of extracts, may be made only in accordance with instructions given by the author and lodged in the Library of NUST Military College of Engineering (MCE) Risalpur. Details may be obtained by the Librarian. This page must form part of any such copies made. Further copies (by any process) may not be made without the permission (in writing) of the author.

The ownership of any intellectual property rights which may be described in this thesis is vested in NUST Military College of Engineering Risalpur, subject to any prior agreement to the contrary, and may not be made available for use by third parties without written permission of the MCE, which will prescribe the terms and conditions of any such agreement.

Further information on the conditions under which disclosures and exploitation may take place is available from the Library of NUST Military College of Engineering (MCE) Risalpur.

## **CERTIFICATE OF ORIGINALITY**

I hereby declare that the research titled "Evaluation of Multisensory MEMS based Accelerometers for Real-time Structural Dynamic Response " my own work and to the best of my knowledge. It contains no materials previously published or written by another person, nor material that to a substantial extent has been accepted for the award of any degree or diploma at NUST or any other education institute, except where due acknowledgment, is made in the thesis. Any contribution made to the research by others, with whom I have worked at MCE/NUST or elsewhere, is explicitly acknowledged in the thesis.

I also declare that the intellectual content of this thesis is the product of my own work, except to the extent that assistance from others in the project's design and conception or in style, presentation and linguistic is acknowledged. I also verified the originality of contents through plagiarism software.

Author Name: Muhammad Yasir Gul

Signature: \_\_\_\_\_

*This thesis is dedicated to my family.*



## **ACKNOWLEDGEMENTS**

Firstly, I would like to thank Allah for helping me to get through and blessing me with the patience and success to reach where I am today.

I am grateful to my Supervisor **Dr. Muhammad Rizwan** for his sincere help. I am also thankful to my GEC members **Dr. Muhammad Shahid Siddique** and **Dr. Bilal Ahmed** for their never-ending help and mentoring at every stage of this research. Without their guidance and motivation, this research would have never been possible. I am also very thankful to my friends **Engr. Wahaj Asif, Engr. Abdul Rehman, Engr. Husnain, Engr. Huzaifa, Engr. Ahmed and Engr. Zafir** for always being there for me in this journey.

Last but not the least, I am grateful to my family members, without their prayers and support, I would have never achieved anything.

## ABSTRACT

Due to advancement in sensing technology and IoT in the last few decades, Intrusion Detection System (IDS) and vibration-based health monitoring of infrastructure (SHM) techniques have gain relevance in structure integrity and safety assessment. While complicate instrumentation and high cost are the major obstructing factors for broad adoption. Right now, SHM is just available for strategically important structures. Therefore, research industry has been working on development of techniques to minimize multipurpose system costs and increase both practicality such as multisensory, wireless, mobile, distributed, smart, remote, and diverse detection mechanisms.

Smartphones having processing power and standalone power supply with multiple integrated sensors, stand out for their potential as SHM module due to the combination of their attractive hardware and software environment. They can create a smart and participative sensor network of numerous structures using their ability to communicate with the web. Such decentralized and self-governing SHM structure established up by crowdsourcing power supplied by people may also be adhered to even by extremely limited resources in terms of equipment and manpower.

How engagement of these smart gadgets in SHM framework will bring several challenges along with many opportunities for public to become involved. In public-initiated SHM scenario, administration has little or no control on sensor instrumentation and operating schedules, and the gathered data is susceptible to alter based on the measurement circumstances. As a result of the sensor setup relying on smartphone user's choices and behaviors, mistakes might arise from configurational errors as well as lack of knowledge in geographical, temporal, and directional uncertainty. Moreover, there is a possibility the smartphone carrying user and as a result, vibration properties detected by smartphones may be altered owing to the human biological system. Some old technology smartphone sensors, on the other hand, have a lower quality and are prone to higher noise levels than traditional high-fidelity sensors. To address such uncertainties there are many problems yet to be solve, an in-depth study should be carried out for behavior of sensor studied and evaluate under different testing facilities and decide for acceptable errors.

In this dissertation we will test validate and evaluate smartphone-based Micro electromechanical (MEMS) accelerometer for low cost and user-friendly SHM approach. From current analysis we determine that the proposed sensor is extremely suitable for monitoring earthquakes effects. According to the evaluations conducted in this study these accelerometers may be used as an accelerograph for vibration-based health monitoring of structure. Sensors were tested for wide frequency bands under different testing facility. As per results MEMS-based technology incorporated in these sensor produces minimal levels of self-noise. Nevertheless, this flat behavior is predicted to remain consistent up to the MEMS accelerometer's resonant frequency, which is far higher than the frequency bandwidth of concern to structural earthquake engineers and seismologist in terms of absolute value. In the clipping tests, amplitude linearity of the relation between the output versus input of the system can be represented using modest values up roll-off level. The sensor's strong performance ensures a constant sampling rate even when used for extended periods of time. Using a shake table to simulate a broad array real frequencies from a unique frequency earthquake, the sensor's performance was ultimately evaluated while dealing with non-stationary signals. Many standard earthquake engineering intensity & effects measurements, commonly include horizontal spectrum acceleration and peak transient response.

## TABLE OF CONTENTS

### Contents

THESIS ACCEPTANCE CERTIFICATE.....	iii
DECLARATION.....	iv
PLAGIARISM CERTIFICATE.....	v
COPYRIGHT STATEMENT .....	vi
CERTIFICATE OF ORIGINALITY.....	vii
ACKNOWLEDGEMENTS .....	ix
ABSTRACT.....	x
TABLE OF CONTENTS .....	xii
LIST OF FIGURES .....	xv
LIST OF TABLES .....	xvii
LIST OF ABBREVIATIONS .....	xviii
<b>1 CHAPTER 1.....</b>	<b>1</b>
INTRODUCTION.....	1
1.1 Background .....	1
1.2 Objectives.....	2
1.3 Research significance .....	3
1.4 Scope of the study .....	3
1.5 Research methodology .....	4
1.6 Thesis layout .....	5
<b>2 CHAPTER 2.....</b>	<b>6</b>
LITERATURE REVEIW .....	6
2.1 General.....	6
2.2 Fundamental objectives of civil infrastructure monitoring .....	<b>Error! Bookmark not defined.</b>
2.3 History and motives for development of SHM in the twentieth century.....	8
2.3.1 Dam Structures .....	8

2.3.2	Bridge Structure .....	10
2.3.3	Installation of Offshore Facilities .....	12
2.3.4	Towers and Buildings .....	13
2.3.5	Installation of Nuclear Plant.....	14
2.3.6	Excavations and tunnels.....	15
2.4	Modern Days Structure Health Monitoring.....	16
2.4.1	Thermal Imaging Visual Inspection .....	17
2.4.2	GPR (Ground Penetrating Radars) .....	<b>Error! Bookmark not defined.</b>
2.4.3	Fiber Optic based Sensors.....	20
2.4.4	Soil Properties Based Sensor.....	21
2.4.5	MEMS Accelerometer .....	21
2.4.6	Comparison .....	22
2.5	Literature Review of MEMS Accelerometer as Low Cost SHM Solution.....	23
<b>3</b>	<b>CHAPTER 3.....</b>	<b>28</b>
	<b>EXPERIMENTAL PROGRAM.....</b>	<b>28</b>
3.1	Methodology.....	28
3.1.1	Stationary input motion.....	28
3.1.2	Non-stationary input motion .....	29
3.2	Model Description.....	30
3.3	Sensors Parameters .....	31
3.3.1	LORDs Accelerometer (G-LINK-200).....	31
3.3.2	BMI160 IMU combining accelerometer and gyroscope .....	32
3.4	Testing Platform.....	34
3.4.1	Actuator .....	34
3.4.2	DOLI Data Acquisition System.....	35
3.4.3	Hydraulic Valve .....	36
3.4.4	Node MCU.....	37
<b>4</b>	<b>39</b>	
	<b>CHAPTER 4.....</b>	<b>39</b>
	<b>RESULTS AND DISCUSSIONS.....</b>	<b>39</b>
4.1	Introduction .....	39
4.2	General performance of the prototyped sensor .....	39

4.2.1	Sensor self-noise .....	39
4.2.2	Flip Box tests .....	42
4.2.3	Transfer function tests .....	43
4.2.4	Sensor linearity and Clipping behavior .....	46
4.2.5	Single and double integration tests .....	47
4.3	Seismic performance of the prototyped sensor .....	<b>Error! Bookmark not defined.</b>
4.4	Input and response parameters.....	50
4.5	Accuracy Assessment Raw Signal.....	51
4.6	Four-storey frame experiment.....	56
<b>5</b>	<b>CHAPTER 5.....</b>	<b>57</b>
	<b>CONCLUSIONS AND RECOMMENDATIONS.....</b>	<b>57</b>
5.1	Conclusions .....	57
<b>6</b>	<b>REFERENCES.....</b>	<b>59</b>

## LIST OF FIGURES

Figure 1 Research Flow Chart .....	4
Figure 2 Thermography sensor for visual monitoring .....	17
Figure 3 Thermograph imagery for SHM .....	18
Figure 4 GPR System Demonstration .....	19
Figure 5 Temperature Shows effect of leakage difference .....	20
Figure 6 Microstructure of MEMS Accelerometer .....	22
Figure 7 SHM Sensors Comparison Plot .....	23
Figure 8 2010 Maule Earthquake elastic response spectrum, Channel 1, E-W, Angol station .....	25
Figure 9 2017 Puebla earthquake elastic response spectrum, Channel 1, N-E, JC54 station. Both spectra have 0.05 damping .....	26
Figure 10 Experimental & Schematic Model of Structure' .....	30
Figure 11 G-Link-200 Wireless Triaxial Accelerometers - LORD Microstrain .....	31
Figure 12 BMI160 IMU combining accelerometer and gyroscope schematic .....	32
Figure 13 Microstructure of MEMS Accelerometer .....	33
Figure 14 BESMAK Shake Table Platform .....	34
Figure 15 BESMAK Dynamic Actuator .....	35
Figure 16 DOLI Data Acquisition Controller .....	35
Figure 17 IDE for DOLI Control System .....	36
Figure 18 Servo Valve .....	36
Figure 19 Microcontroller base Experimental Setup of BMI 160 .....	37
Figure 20 Schematic Diagram .....	37
Figure 21 IDE Node MCU Sketch .....	38
Figure 22 - 12 h Continuous Recording for Noise Test .....	40
Figure 23 - Average power spectral density of MEMS accelerometer acceleration over 12 hours of motionless state .....	41
Figure 24 Sensor data flip-box test. The top plot shows the sensor's positions during the test; the arrow indicates the axis's upward and descending position relative to a level surface. ....	43
Figure 25 Raw data from a 4 mm, 4 Hz sinusoidal input signal. ....	44
Figure 26 Raw data from a 4 mm, 4 Hz sinusoidal input signal. ....	44
Figure 27 Amplitude ratio of Smart phone .....	45
Figure 28 Amplitude ratio of LORD signals .....	46
Figure 29 Sine wave Acceleration plot .....	48
Figure 30 Sine Wave Velocity plot .....	49
Figure 31 Sine wave displacement plot .....	49





## LIST OF TABLES

Table 1 Description of Model .....	30
Table 2 Structure Primary Parameter.....	31
Table 3 G-Link-200 Wireless Triaxial Accelerometers - LORD Microstrain Parameter .....	31
Table 4 BMI160 IMU Combining Accelerometer and Gyroscope Parameter.....	33

## LIST OF ABBREVIATIONS

IDS	Intrusion Detection System
SHM	Structural Health Monitoring
MEMS	Micro-Electromechanical Systems
IMU	Inertial Measurement Unit
CA	Conditional Assessment
MIDAS	Modular Interactive Data Acquisition System
ENEL	Italy's National Entity for Electricity
AGR	Magnox or an Advanced Gas-Cooled Reactor
CSMIP	California Strong Motion Instrumentation Program
PCPV	Prestressed Concrete Pressure Vessel
NII	Nuclear Installations Inspectorate
SGs	Strain Gauges
PIGs	Pipeline Investigation Gauges
RFIDs	Radio-Frequency Identification
GPR	Ground Penetrating Radar
MEMS	Microelectromechanical Systems
CMOS	Complementary Metal–Oxide–Semiconductor
JPEG	Joint Photographic Experts Group
FOS	Fiber Optic Sensor
LVDTs	Linear Variable Displacement Transducers

## INTRODUCTION

### 1.1 Background

Building stock in cities has risen dramatically during the previous two centuries as a result of industrialization and urbanization. Many structures are suffering from structural degradation, damage, and collapse over time due to ageing, fatigue, and natural and man-made calamities. In most situations, engineering design had to assume a fair risk and balance between safety and economics due to the unpredictable and variable nature of structural demand and capacity. Therefore, an estimation of serviceability and required safety measures are crucial for maximizing the performance of these building stocks. Static and dynamic analytic techniques for evaluating the performance of existing structures have developed in structural engineering rules and regulations as a way for predicting and assessing outcomes before and after events. Although these methods depend entirely on mathematical models, experimental data illustrating the structure's true features is missing from the mix. So far, several state-of-the-art mathematical models and real time sensor data, such as vibration-based SHM, have emerged as an essential approach that combines analytical and experimental knowledge to analyze the requirements for serviceability.

Vibration-based SHM has been widely investigated in the field of civil structure engineering during the last two decades because of advances in sensing technology and computer capability. Adopting systems identification method (IDS) on a comparative basis engineers can use SHM as integrity and safety evaluation tool for buildings, bridges, dams, etc. Adding to this, finite element models updating with monitoring data provides an appropriate framework for verifying and calibrating models with real-world data and enhancing analysis accuracy. Decisions on current civil infrastructure investments may be made more intelligently as physical and digital representations of such assets become increasingly interconnected. Ongoing research

for such technology advancement can bring a revolution, where data acquisition will be done through automated controllers and connected sensors for civil infrastructures

Vibration-based SHM, despite its many benefits, requires a significant amount of time, money, and effort to implement and maintain in the field. It takes a long time and might be difficult, risky, or even inapplicable to put sensors and cables on civil infrastructure. Emerging methodologies, such as non-contact-based vision sensing, GPS, laser interferometer, displacement, and more, are being used to address these practical issues. Similarly, other technologies e.g., IOT based gadgets, smart sensor networks and wireless based systems are now widely investigated to have reliable and remote access to sensors, such as strain gauges, accelerometers, and tiltmeters. Besides sensors connected to single acquisition system, a decentralized heterogeneous, but monolithic system can collect numerous structural responses characteristics, such as displacement, acceleration, tilt, strain, and more.

In addition to the recent advancement in engineering and measurement science, smartphones have also emerged and started contributing toward the field of communication. Their internal hard-drive, embedded batteries, sensors and processor make them a standalone potential compound for vibration-based health monitoring instruments. It is by default, intelligent, mobile, ubiquitous and sustainable. Soon after some research-based release, such smart gadgets will be introduced as seismic monitoring modules as explained in current study for vibration-based health monitoring systems.

Despite the many benefits of newer technology, the uncertainties and errors that resulted from public engagement in SHM made it difficult for use. Such decentralized sensing system and the operating schedule are not within the control of the platform developer, as is the case with most monitoring systems. As a result, residents are encouraged to take the lead in monitoring structural vibrations in accordance with their own choices and activities. These SHM-related uncertainties due to self-governance and auto-control capabilities have taken on new dimensions to the vibration-based sensing and health monitoring platform. But by studying the deep inside behavior of concurrent to earth quake and structural health monitoring we can cope up with these uncertainties. So, this decertation will deal with evaluation of Smart phone behavior under seismic or any dynamic excitation for structural dynamic response.

## **1.2 Objectives**

The aim of this research work is to design a methodology for smartphone to collect SHM based acceleration or vibration data collection. Using this methodology, a series of experiments performed on embedded sensors for evaluation of its performance under stationary and nonstationary conditions. After experimentation acquired results are compared with commercially available sensor for SHM to grade its performance. The objectives of the study include:

- i. Develop of framework to utilize MEMS base accelerometers for SHM as a low-cost and user-friendly solution
- ii. Evaluate the sensors using signal processing and modal analysis technique

### **1.3 Research significance**

The civil infrastructure plays very important role in economic development and societal activities of society. Many wealthy countries throughout the globe have made significant investments in this kind of infrastructure. The ageing and degradation of such assets is a worldwide issue. SHM can be the tool to monitor effect of these processes on building performance. But due to high cost and complex instrumentation SHM is only available for strategic important structure, while major part of above-mentioned investment is concurrent to common buildings. So the significance of current study to develop SHM technique which make such facility available for common structures.

### **1.4 Scope of the study**

The scope of this study is to develop and design sensor application guidelines along with its evaluation, whether purpose sensor embedded in smartphone is suitable for its deployment as a monitoring tool for structural system subjected to seismic event and any other dynamic loading scenario. To provide guidelines we are using readily available software applications and hardware modules which can be acquired through over the shelf facility. And for evaluation part we are following standard testing procedure for vibration-based MEMS behavior & performance analysis. This testing is a real-time experimental procedure executed under the controlled laboratory bound condition. This evaluation is totally based on data driven approach for stationary and non-stationary input signals. An integrable and a low power inertial measurement

unit (IMU) BMI-160 was used in this study that provides accurate angular rate (gyroscopic) and acceleration mensuration. Experimental data history is then compared with Parker-LORD accelerometer results under similar conditions for validation, which bring confidence to the users regarding their application in health monitoring of infrastructures.

**1.5 Research methodology**

Flow chart of research methodology is as below:

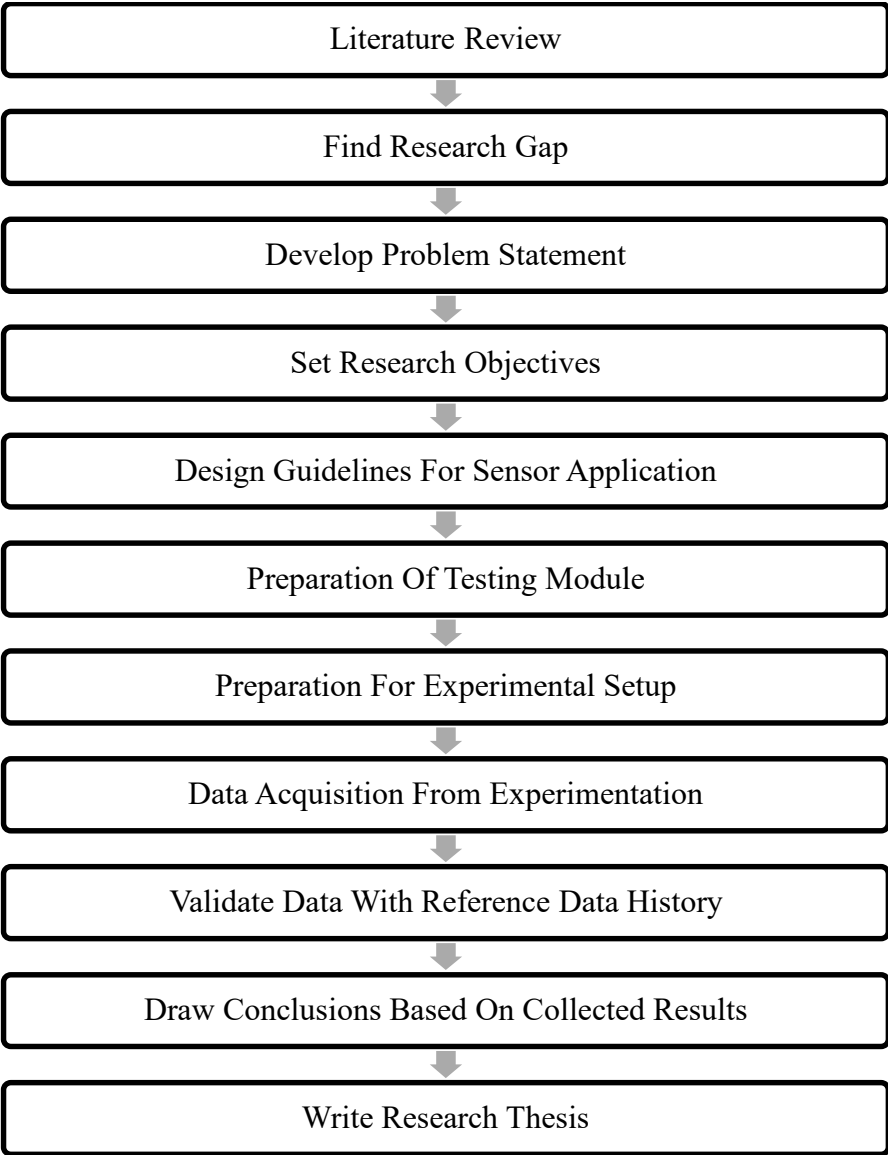


**Figure 1 Research Flow Chart**

## **1.6 Thesis layout**

The research undertaken to address the aforementioned objectives is presented in five chapters:

Chapter 1 “Introduction” explains the importance of Structural Health Monitoring (SHM) and its limitations and uncertainties, research objectives, research significance, scope of the study, and research methodology followed by thesis outline.

Chapter 2 “Literature Review” a brief revision on the previously related research regarding SHM Application has been presented. The literature review also includes that with advancement in technology how SHM evolve over the period of time and new opportunities along with different challenges bring the revolution in stream.

Chapter 3 “Experimental program” discusses the test procedures and methodology. This chapter presents the instrumentation plan, testing techniques, SHM data collecting, and relevant aspects pertaining to this research investigation.

Chapter 4 “Results & Discussion” includes analysis and discussion for results to evaluate the behavior of Smartphone embedded accelerometer as seismographer under dynamic loading scenario. Its performance under real-time seismic activity has also been presented.

Chapter 5 “Conclusions and Recommendations” summarizes, in a nutshell, the findings of this investigation as a whole and remarks for further studies.

### LITERATURE REVEIW

#### 2.1 General

Civil infrastructure system is an indispensable component of a society, which comprises of buildings, tunnels, vehicular bridges, pedestrian, factories, and offshore petroleum installations, nuclear power plants, structures of historical significance, ports, and geotec structures. Therefore, inspection and maintenance programs using reliable monitoring systems may even be required by legislation depending on the structure's significance (ownership, usage, danger, and hazard). Real-time, and automated technologies are now being used to restricted and intermittent inspection techniques in order to improve maintenance and inspection efficacy. The oil sector, big dam operators, and roadways authorities have been major movers in this field, and their installations have garnered the most research efforts and attention. Commercial and residential buildings have gotten comparatively little attention because of the duties and repercussions that owners may face if they discover that their buildings are in bad condition. After educating or coercing owners through building control regulations (legislation) or premium insurance, structural health monitoring can only be applied in certain situations. (Chang, 2000). The fact that, apart from some kinds of private housing and public, every building is unique and need different strategy for SHM, which make it a challenging task. If you don't have type testing or costly qualification processes, you don't have a reference point. Consequently, SHM for engineering structures has the unusual characteristic that a significant portion of the system must be focused on an ongoing assessment of structural health and performance. (Brownjohn, 2007)

#### 2.2 Civil infrastructure monitoring's primary goals

(Ross, 1995) found out what kinds of situations would necessitate structure monitoring, such as :

- i. Modification in the existing buildings design,



- ii. Structural monitoring exaggerated by external works,
- iii. Monitoring the behavior while dismantling and demolition,
- iv. Infrastructures subject to degradation of materials or long-term movement,
- v. Modification in the existing design depending upon feedback or experience based future designs.
- vi. fatigue and failure assessment,
- vii. innovative building methods
- viii. evaluation of the structural integrity after the earthquake,
- ix. reduction in construction and increase in maintenance requirements are two trends that are occurring, and
- x. shift in design philosophy to focus on performance-based design.

In the past, health monitoring of structures (SHM) relied on data gathering, processing, and diagnoses. Simple visual inspection and evaluation of structural component (cracking, spalling, and deformations) on a regular basis could be considered SHM. The goal of this study is to develop data collection and processing systems that are efficient and accurate while also removing or replacing the unreliable and subjective human factor. However, in recent years, some researchers have started to concentrate on, or at least acknowledge (Fanelli, 1993), the necessity for a comprehensive view to SHM optimization. Innovations in SHM have typically targeted specific aspects of the larger Structural health monitoring standard in the past.

Using time series data the analytical model of the structure is monitored continuously by SHM. The SHM pulses are obtained from based on live vibration activity as well as from Sudo-static processes that change slowly, like solar insolation cycle. When a reference function has been constructed, SHM processes are used to look for instances where output signals deviate from predictions made using the established form.

One of the many branches of SHM is "condition assessment," or CA, a comprehensive evaluation performed only once on the structural system. In real time, Monitoring should really be able to execute some CA, but the SHM system is more likely to launch and aid a follow-up enquiry CA with the information it collects.

Although there has been significant advancement in SHM, it remains difficult to restore reliable ingredient structural real-time information utilizing system identification. It is not anticipated that SHM advancements for civil infrastructure would have an essential quality for angular position and quantification anytime soon. While there is a wealth of literature on resonance-based damage identification (M. & Schevitz, 1996) the viability of VBDD for live civil structures has only been proven in simulation-based studies and the trials performed in a controlled laboratory environment, such as the (Maeck, Peeters, & de Roeck, 2001)

Short-term objectives are therefore relatively pessimistic and concentrate on automatically delivering a trustworthy and early notice of a developing or fresh structural collapse coupled with limited diagnostics.

### **2.3 Background for development of SHM in the twentieth century**

Big-scale building initiatives, like long-span suspension bridges, large dams, and Installations for producing and refining oil and gas that are located far out to sea, have given rise to significant developments in SHM. A more modern "standard" known as structural health monitoring (SHM) emerged from activities earlier referred to as structural health or simply monitoring. Short-term goals are therefore rather gloomy and center on automatically providing a reliable and early signal of a growing or fresh partial collapse paired with limited diagnostics. SHM may be traced back to the latter part of the twentieth century, when the use of recording and formal structural monitoring instruments began and gained momentum with the era of digital information storage and computational data collection. The official deployment of SHM technique to other infrastructures, such as dams, which has been a necessity in the UK, at least over several decades, has been eclipsed by the attention recently in the civil SHM industry that has been given to bridges (Ross, 1995).

#### **2.3.1 Dam Structures**

Dam inspections were mandatory in the United Kingdom after a collapse of a 30-meter embankment killed 254 people in Sheffield in 1864. Hence, the Reservoir Law of 1975, the most recent piece of law in the UK, charges a supervising engineer with maintaining constant watch over reservoirs or dams, including the recording and analysis of operations (DETR, 2001).

Therefore, dams have historically been the best mechanism for the necessary implementation of Health monitoring, as well as other buildings may gain a lot from studying their design and operation. The engineering discipline of dam construction, SHM is the equivalent of surveillance, and ANCOLD (1994) and the International Commission for Large Dams provide good descriptions of what this implies in more depth about structured monitoring (ICOLD, 2002) There are many components of the contemporary SHM paradigm in place, such as:

- i. a variety of instruments designed to provide data on safety-critical responses, together with visual checks,
- ii. automatic data gathering,
- iii. intelligent comparison of data to known behavioral patterns and the detection of anomalies.

In the United Kingdom, item (iii) falls under the purview of the supervisory engineer, and research on artificial intelligence (AI) applications for this role has been spearheaded by the ISMES division of Italian energy company ENEL. To briefly recap the extent of the ENEL reservoirs monitoring programme (Fanelli, 1992) describe it because it uses nearly all of the tech being considered for other initiatives. When it comes to ENEL's list of structures, transducers are installed in every major dam. These transducers are periodically activated by a central processor to assess static "structural impacts," for example:

- i. absolute or relative displacements: For concrete dams, lateral crest displacements are particularly crucial.
- ii. tension adjustment for temperature (for concrete dams).
- iii. measuring uplift forces, such as those that contributed to the Malpasset Dam's collapse in 1959; and
- iv. rate of seepage.

Additionally, transducers are turned on to capture "external impacts" that the dam responds to by altering its structural characteristics, such as

- i. level of water
- ii. temperature of structure
- iii. meteorology based conditions.

The acceptability of the structural effect changes is assessed considering environmental variation. Deep understanding of the dam's structural behavior is necessary for this decision. This is typically the responsibility of a supervisory engineer, although advancements in the monitoring system have replaced this. According to (Fanelli, 1992) since 1985, 200 dams in ten different nations have had data managed via the commercial application of the info system known as MIDAS.

Because of this system's shortcomings, ENEL anticipated the need to combine formal tools like Supplementing MIDAS's formal data with anecdotal evidence and expert engineering opinion. (Salvaneschi, 1996) further describes the development of two artificial intelligence programs, DAMSAFE and MISTRAL. MISTRAL a proper system designed to consider the consequences with or without link to influences. In the first scenario, comparison and anomaly detection are done using statistical or physics-based models, however in the second scenario, aberrant behavior can still be detected. Engineers can use DAMSAFE (Comerford, 1992) to help with Risk management for dams. It's completely non-online and functions more like an "expert system" because it incorporates previous knowledge into its body of knowledge. But today it has mostly faded from public awareness, although it is being refined in other nations for use in bridges and dams. (Wu & Su, 2003)

The purpose of dam SHM is to monitor dynamic response for two reasons. Firstly, earthquakes pose a severe risk to the security of dams; every opportunity is used to recalibrate models and simulate to understand the influence of seismic activity on the dam behavior. (Severn, 1981). Second, estimations of dynamic properties acquired from environmental monitoring (Proulx, n.d.) or purposeful induced vibration (Bettinali, 1990) offer a way to monitor the structural response as indicators of structural health.

### **2.3.2 Bridge Structure**

In the past, monitoring programmes of bridge have been used to comprehend and at last, load-structure-response chain models can be calibrated (Bettinali, 1990; Severn, 1981; Wu & Su, 2003). Among the first documented instances of bridge monitoring, by (Bettinali, 1990), was carry out on the Bay Bridges and Golden Gate in San Francisco in a measuring period of

elaborate programme of the many components during their making to evaluate the probable consequences of an earthquake and dynamic behavior. Again, focusing on vibration data, Washington State University (1954) details how they kept an eye on the original Tacoma Narrows Bridge during its tragically short existence due to its vulnerability to wind-induced instability, but with a legitimate concern about the building's integrity. Since concerns about wind-induced reaction and possible instability, like at Humber, have prompted all previous long-term span bridge monitoring operations, Tacoma's Narrows experience is highly relevant (Comerford, 1992). Despite significant advancements in the knowledge of bluff-body aeroelasticity, long-span bridge aerodynamics continue to surprise (Maeck et al., 2001) and the most sophisticated SHM systems employed in civil infrastructure are expensive, but they are justified by their strategic importance and monetary return. Permanent bridge surveillance system has evolved into Structural health monitoring systems over the past ten years and have been used in significant jobs in Hong Kong, Japan and most recently the USA. As an illustration, the wind and SHM scheme (Wu & Su, 2003) the Cross walk of Lantau Fixed installation has prompted studies on SHM in Hong Kong, both in terms of the structural performance themselves as well as SHM methodologies. Additionally, SHM system development and research may be advanced by long-span bridge monitoring systems. To ensure the safety of the public, modern long-span suspension bridges undergo rigorous inspection and maintenance schedules. This means that significant deterioration and damage to the structural elements are more likely to be spotted visually than by a SHM system, which would require advanced concentration of sensors to detect it. It is unlikely that global SHM algorithms will detect smaller issues, such as the loss of a major cable or the tension of a deck part, or localised ones, such as a failed bearing or foundation settlement, without a significant number of strategically positioned sensors. The best monitoring strategies for typical short-span bridges would be less flashy but ultimately more beneficial advancements of SHM. There has been research into the efficacy of full-scale testing for assessing highway bridges having short span. (Salane et al. 1981; Bakht & Jaeger 1990), and there are apparent prospects to apply similar methods to automated monitoring exercises. Smaller bridges have a global reaction which is more responsive to flaws, less frequent eye inspection, and a true place for SHM systems (Alampalli & Fu 1994). The BRIMOS system (Geier & Wenzel 2002), which tracks dynamic features, has been employed in European research on shorter-span bridges. Due to the focus of research in Australia on typical very

small-span highway and railway bridges, a commercial product known as the "Bridge Health Monitor" or HMX (Heywood et al. 2000) was developed. (Heywood et al. 2000) was developed. This product is configured to capture picked wave patterns of vehicular responses whilst also trying to log statistical data of isolates due to such events. Bridge management programmes and bridge improvement projects, which call for some sort of validation and even make it the contractor's responsibility to assure the success of the upgrade, provide direct incentives for monitoring (Yanev 2003). Refurbishments of the Wye and Seven Bridges in the United Kingdom and Singapore's Pioneer Bridge (Flint and Smith 1992), including the Severn Bridge and Wye Bridge in the United Kingdom, and the Tamar Bridge in Cornwall (Brownjohn et al. 2003a, b) are such example. Similarly, investors may be certain that they are receiving a fair price and that the property will be in pristine shape when the concession ends if monitoring is a part of the construct, own, manage, and transfer arrangement.

### **2.3.3 Installation of Seaward Facilities**

Fixed steel or concrete manufacturing installations, which are subjected to harsh environmental stresses, main energy use, and the subsequent finding of Offshore Petroleum resources, both of which saw tremendous growth in the '70s. Vibration-based diagnostic devices have seen a surge in popularity as an alternative to costly and dangerous diver inspections, which are now required by law (Veritas, 1977). The Norwegian Oil and Gas Directorate requires this inspection "to assure the efficacy of the massive pile structure of both the base and their platform."(Spidsoe, N., Berg, S., Hoen, C. & Beck, 1980), platform and environmental performance (E- and P-) data were gathered by the platform operator. Several installations here on Norwegian continental shelf had their dynamic properties and load-response mechanisms identified as a result of the research. An array of methodologies for ambient response system identification emerged around the same time, serving as forerunners to the present study of "Ambient modal identification." (Peeters & De Roeck 2001a). Dynamic parameter estimations were improved by using the maximum entropy technique and random decrement (Yang, 1981) on data obtained from the platform as part of vibration-based diagnostics. While it was found that identification was achievable in some cases, most of these investigations concluded that it could only be done under carefully monitored conditions or when there had already been significant structural damage.

Structural Monitoring Limited concluded that techniques will not be enhanced until the offshore industry expands an integrated concept embracing (M, 1981). development, with help of contractors, about an efficient instrument for inspecting, maintaining, and keeping tabs on. Assuming such potent resources already exist, they would presumably be kept under wraps for reasons of confidentiality.

As a result of structural adjustments, offloading of stores, hydraulic movement in processing plants, and drilling activities the building is a quasi-system with constant variations in mass characteristics. Unknown to the damage detection system, a different structural module was installed, which led to an incorrect identification of a failing structure member.

### **2.3.4 Towers and Buildings**

When earthquakes and storms struck, the desire to better understand how buildings performed led to the development of building monitoring systems. Testing for low-amplitude vibration yielded the first insights into low-amplitude dynamic response (Hudson, 1997). Long-term monitoring has always been necessary. In order to learn how a structure reacts to a common, but not ultimate, large-amplitude loading event. The California Strong Motion Instrumentation Program (CSMIP) is in charge of overseeing the state's obligatory structural monitoring program. (Geological Survey California 2003), levies on owners of building to pay the and operation and installation of strong ground motion devices on buildings of the building owners' selection. Data on structural health can be useful, but the goal is to offer information on ground acceleration and to enhance the design of structures in response to these motions, rather than providing information on structural health. Earthquake engineering research has always revolved upon determining the structure performance at full size. Earthquake engineering research has always revolved upon determining the structure performance at full size. It is important to consider the occupants' well-being while determining the wind loads of future, even taller, apartment buildings in Singapore (Balendra et al. 2003). Recent large earthquakes, such as those in Kobe and Northridge, have provided additional impetus for the SHM of buildings, as relevant information about the situation of structures is critical for determining their safety and the extent to which repairs are necessary (Mita 1999). When SHM triggers and then assists CA, It exemplifies the use of an integrative approach to SHM, which incorporates unique sensing

devices that are autonomous and independent from one another, embedded systems, communications, data management, and mining. (Lynch, 2005).

The technique to SHM proposed by Jeary and co-authors (Jeary, 2001) is a straightforward and pure approach to the standard SHM paradigm, and It's the end product of twenty years of extensive monitoring and testing of major structures. Due to the emphasis placed on making a profit, the method's specifics are being kept secret from the public. The system basically uses high-end accelerometers and other data-gathering devices to monitor fundamental mode damping and building tilt, as well as improvements in random decrement methodologies. It has proven possible to diagnose structural issues in Hong Kong's skyscrapers using these two metrics. When compared to the vast majority of SHM systems that rely on tracking natural frequencies, this application of dampening for SHM is significant.

### **2.3.5 Installation of Nuclear Plant**

Smith (1996) presents an overview of the UK's civil nuclear reactors' inspection and monitoring regimes. Structural response measurement instruments are used to validate calibrate and validate designs while testing of performance and contribute in monitoring normal operations for reactor safety-critical structural components.

The United Kingdom typically has two reactors per nuclear power facility, both of which are Magnox or advanced gas-cooled reactors (AGR). All existing AGRs and Magnox reactors rely heavily on the durability of their precast concrete pressure vessels (PCPVs), which contain the reactor core and main coolant. The pressure containment and protection vessel (PCPV) is often a very thick cylindrical vessel with extensive steel reinforcement, including redundant spirally coiled ou pas post-tensioning wires that maintain the vessel in a continuous compression condition. In accordance with the Nuclear Installations Act, the Nuclear Installations Inspectorate (NII) issues operating licenses for nuclear reactors. (Smith 1997). PCPVs must be tested and operated before they can be licensed or renewed. This is a condition of awarding or renewing the license. It is the licensee's responsibility to show if the plant is able to fulfill the purpose and nuclear safety duty in a "safety case" provided to NII.



Three-year 'statutory outages,' or planned shutdowns, are required for comprehensive reactor inspections. NII requires a report from a competent appointed examiner (AE) before the reactor may be restarted. This examiner (AE) has a duty similar to that of a dam's supervising engineer but is supposedly independent of the licensee and NII. The AE will include the outcomes of all tests and inspections, as well as any structural or performance data gathered before to the outage. This report is presented as part of a licensee's app to restart the reactor.

Vibrating wires strain gauge (SG) data is less important than temperature measurements since they are not as vital to determining the overall operation of the machine. In-service structural behavior analysis is necessary for calibrating and improving the performance of temperature-dependent structures. While performing the analytical simulations, strain data is mostly used for post-processing. Online monitoring of response of a structure so far has not had a significant impact on the PCPV's ability to track its own health in the United Kingdom. As strain data are regularly logged and reveal unambiguous signs of operational changes, there is a lot of potential. Applications like this could be spurred by the finding of a 15-cm void within pressure chamber heads for Besse-Davis reactor (Cullen, 2002).

### **2.3.6 Excavations and tunnels**

In order to make sure that the deformation of the tunnel is in acceptable range stability-wise, and in terms of potential effects on or from nearby buildings, tunnel monitoring (Okundi, 2003) is carried out. While stress - strain curves can be quantified, deflections are of primary importance in this context. Many heritage structures, such as the Mansion House in London, are under constant surveillance while an underground railway extension is being built nearby, in Australia, listed nineteenth-century mining facilities are being watched closely as explosive blasting occurs at a nearby open-cast mine (Roberts, 2003). In these short-term ground surface monitoring operations, all the same equipment is used as in long-term systems.

As a result of building operations taking place on the surface, Singapore requires tunnel deflection monitoring equipment (Tan & Chua 2003). A wireless remote monitoring system is used to monitor the surface and tunnel deflection, where threshold crossings of deflection parameters can be communicated over Internet or in the form of text messages to operators.

True SHM systems can benefit geotechnical constructions and offers a simplest case study situation. For example, the use of SHM systems has been highlighted by a study (Loh 2004) on a fatal tunnelling excavation collapsed in Singapore in April 2004. Post-accident examination of recordings wireless remote sensing and monitoring technology is used for data transmission in surface and tunnels deflect monitoring, with Internet service or text message to operators informing them when threshold deflection parameter crossings have occurred. According to data obtained from the instrumentation, there had been abnormal motions in the dig wall for at least two months prior to the catastrophe. A small amount of online processing, along with an automated alarm, might have simply and accurately detected such sluggish and monotonous movements, as well as any acceleration. Wireless automated surveillance in Singapore has grown in popularity as a result of this occurrence.

Civera et al. (2003) created a MEMS inclinometer which was used to electronically broadcast the danger of earth tremors near quarry excavations, LaHusen and while Reid (1998) employed telemetry to watch the Cleveland Fence landslide for 5 years, both groups applied SHM technology to landslide detection.

## **2.4 Modern Days Structure Health Monitoring**

Modern days technology leading SHM of commercial and civil structures to real time which helped to avoid the economic loss and improve living condition. Bridges, buildings, and pipelines are all examples of constructions that need to be monitored to ensure their long-term viability due to time or natural forces, e.g., earthquake, wind deterioration, and so on. Most structural health monitoring systems offers expensive, non-invasive, and cumbersome solution to be retrofitted into existing structures. But the advancement in technology is trying to fight with scenario using low cost and reliable solutions such as The use of Pipeline Investigation Gauges (PIGs), radio-frequency identification (RFIDs), subsurface interface penetration radar and acoustic sensors. Long-range subsurface interface penetration radar are capable of identifying screw ups, but they necessitate full human interaction. However, PIGs can only detect faults at a limited distance and require more human participation. When surfaces vibrate, acoustic sensors pick up frequency oscillations but aren't able to detect low frequencies. Reliability, robustness, retrofit ability, and cost effectiveness are all criteria that must be met for structural health

monitoring systems, and these techniques fall short. Newly established monolithic manufacturing technologies known as Microelectromechanical systems (MEMS), complementary metal–oxide–semiconductor (CMOS) have made it possible to produce accelerometers that are both small and inexpensive. Wire bonding of the MEMS accelerometer's readout-IC (ROIC) and capacitive comb structure is common. New technologies like monolithic microsystems, in which microelectronic devices are integrated into one piece of silicon without any or little post-processing are being used. Because of this monolithic integration, it is possible to mass-produce a system that is low-cost, low-power, small, resilient, and high-performing in millions of units. It is non-invasive and retrofittable since it uses real-time vibrational structural analysis to monitor acceleration changes. Data converters, pre-amplifiers, filters, and other components are required for MEMS accelerometers to operate at low noise and low power. Sensor approaches for real-time SHM, such as those described above and others, are discussed in literature study.

#### 2.4.1 Thermal Imaging Visual Inspection

Simplest example of external image sensors, but not unsuitable and real time for underground/hidden constructions like tunnels. (Resende et al., 2022). Infrared thermography could be used to detect leaks in pipelines. In some cases, temperature variations in the nearby area can reveal leaks. Leaks of hot water in the vicinity were discovered using infrared thermography. Thermography is based on the premise that when water leakage through the underground pipe, it alters the thermal properties of soil, making it more reliable heat sink than the dry soil around it.

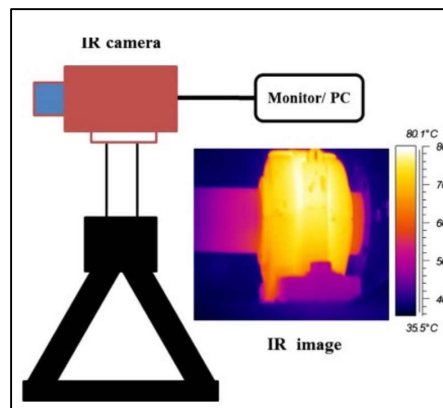


Figure 2 Thermography sensor for visual monitoring

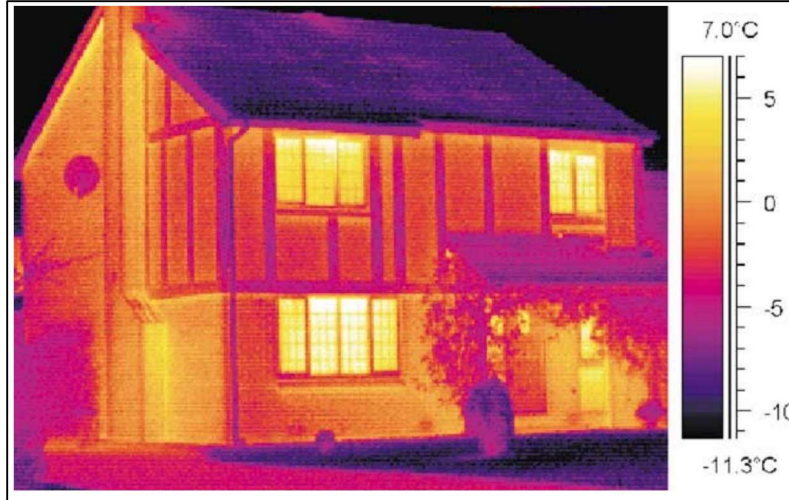


Figure 3 Thermograph imagery for SHM

Thermal anomalies above pipelines can indicate water leaks, and infrared scanners are employed to detect these. Scanners are available in two configurations: hand-held and vehicle mounted. A video of the area is recorded by the thermographic sensor. JPEG (Joint Photographic Experts Group) and other picture formats are then used to save the video. Image processing procedures such as thresholding and binarization are then used to these images. The `rgb2gray` procedure performs a thresholding on the photos. The pixel values in the degraded image are used to classify the image. In the scanned environment, an image of thermal mapping is obtained and used to detect various irregularities in pipes, as well as structures such as bridges and buildings.

#### 2.4.2 Subsurface Interface Penetration Radar

subsurface interface penetration radar provides an alternate method that can be installed beyond the confines of the building for analyzing the subsurface pipes instead of excavating (Resende et al., 2022), able to cover several miles of inspection per day, despite the fact that human involvement is still required and real-time monitoring is not possible with this technique. At a frequency between 10MHz and 2.5GHz, ground penetrating radar (GPR) transmits electromagnetic energy into medium. Until it comes into contact with an electric interface, the pulse passes through the medium. As a result, a few of the energy is reflected, while the remainder is carried forward. An anomaly in the structure can be detected by receiving the reflected energy at interfaces among material with distinct dielectric characteristics and conductivities. Waveforms representing the magnitude and elapsed times between the

transmission and reflection of waves are created from the gathered reflected energy. Ground penetrating radars typically collect the following types of information:

- i. Strength Reflection Variation.
- ii. Arrival time difference of specific reflections.
- iii. Source wave distortion
- iv. Attenuation of signals

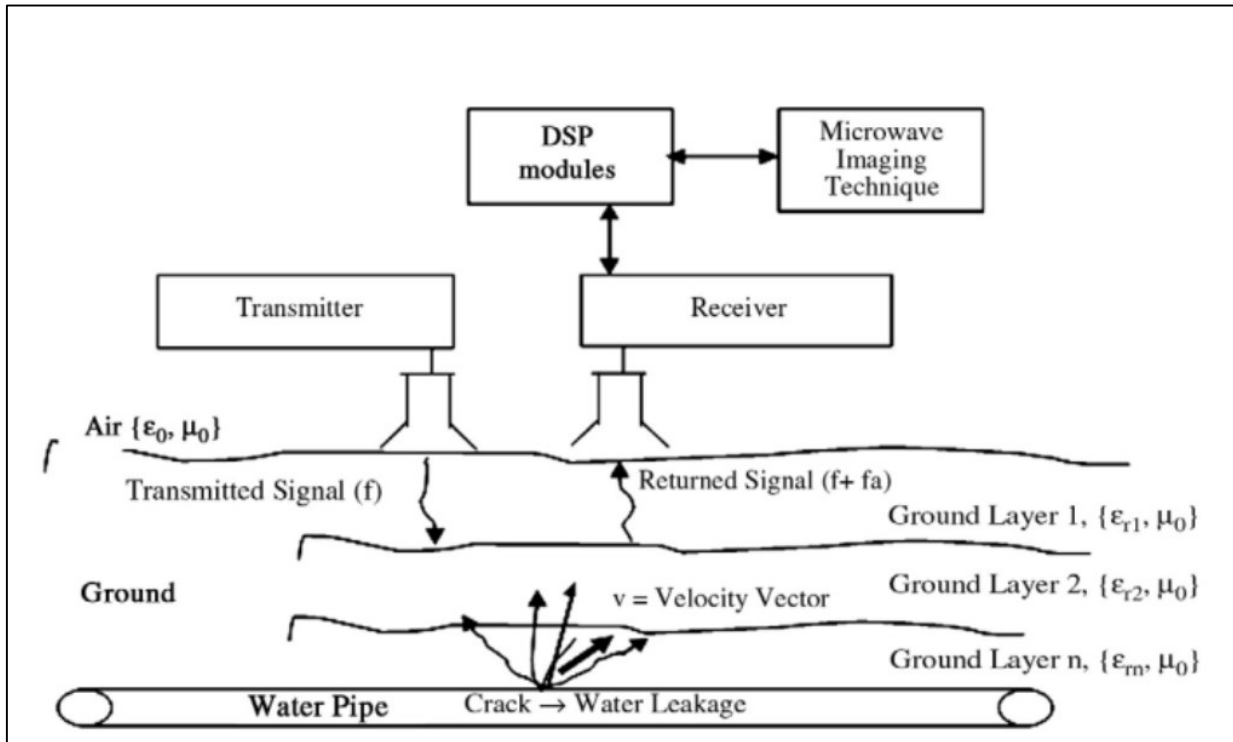


Figure 4 GPR System Demonstration

It is possible to utilize ground penetrating radars (GPRs) to locate steel reinforcements corrosion inside the concrete deck using distinct signatures of GPRs. Since the earth's layers have differing electromagnetic properties, GPRs can be used to detect leaks in pipeline networks, i.e., conductivity  $\sigma$  and distinctive constant  $\epsilon_r$ . Figure 4 GPR System Demonstration shows that the ground layer 'n' is usually near to the pipeline network. The DSP module and microwave imaging technology are then used to extract and distinguish relevant data from the rest.

### 2.4.3 Fiber Optic based Sensors

Fiber Optic Sensors (FOS) can also be used to monitor the structural health of a building. Installation of a fiber optics system (FOS) allows for optical based reflectometry to be employed for the diagnosis of structural defects through the use of dispersed strain profiles. generated by Raman or Brillouin scattering (Bremer et al., 2016). Localization accuracy is measured in micrometers (m), but the FOS system requires expensive interferometer-based sensors, which have an effective range of only 100-200 miles (160-240 kilometers). As a result, it's inappropriate for structures that span long distances above ground due to the system's one point of failure: the fibre. When the liquid is compressed, as seen in Figure 5 Temperature Shows effect of leakage difference. Cooling takes place in the nearby region of the pipeline. The Joules-Thompson effect is then used to detect leaks. In an adiabatic state, the fluid's temperature decreases as a result of any pressure changes, such as those induced by leaks. The temperature change is subsequently detected by the interrogator, which leads to the leak detection and location.

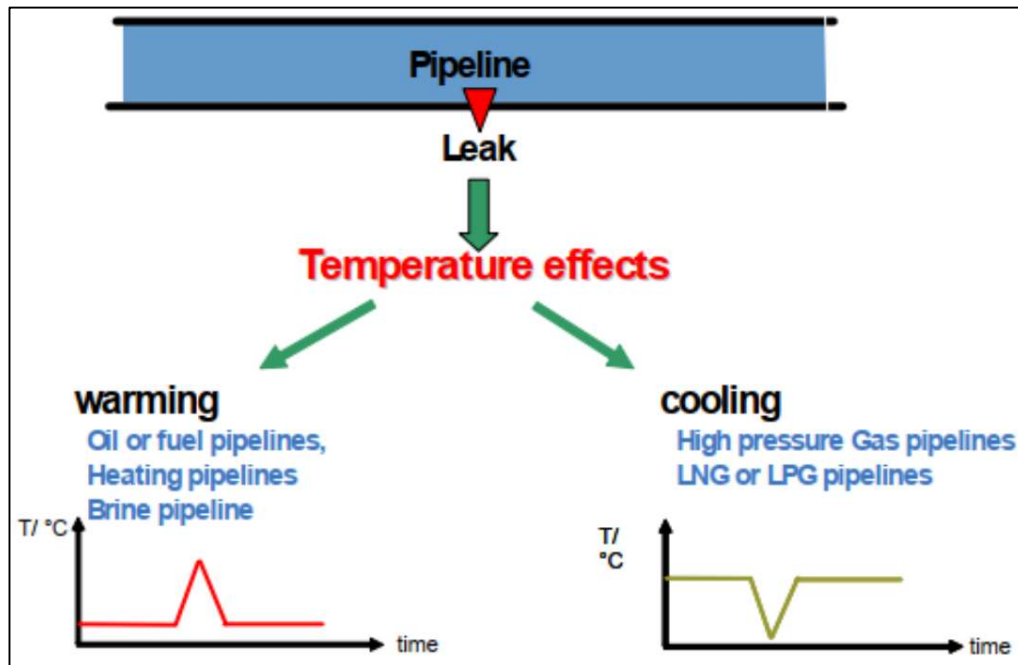


Figure 5 Temperature Shows effect of leakage difference

According to standard formulas, temperature changes of 0.5oC per bar of pressure (P) cause significant temperature changes. Oil, brine, and other heating system fluids must be transported at a greater temperature than the earth. Therefore, even a minor leak raises the temperature around the pipeline. Any time a local hub develops along the detecting cable, there's a leak.

#### **2.4.4 Soil Properties Based Sensor**

In the event of a pipeline leak, it is possible that the local soil and ecosystem could be altered. Humidity, temperature or dielectric can all alter (soil bulk permittivity) (Bremer et al., 2016). There are times when the dielectric constant of soil increases due to a water leakage, given the fact that the dielectric constant of water is relatively greater. Sensor data are sent to a central hub, where they are checked against predefined steady state value and an anomaly alerted if there is a difference. Detection, on the other hand, is not that simple. When the soil's qualities are unevenly distributed across a vast area, the accuracy suffers. The other parameters also have an impact on its effectiveness such as the properties of neighboring soil, kinds of organic matter, temperature, saltiness, form, and even when the soil was generated. The reduced sensitivity of SPS makes it less effective in detecting pipeline leaks with big diameter pipes because it needs a bigger anomaly before it is dispersed by the ambient air.

#### **2.4.5 MEMS Accelerometer**

It is difficult to implement many of the above-mentioned strategies on legacy systems since they are invasive in nature. In addition, some of these methods are real-time, yet they are vulnerable to intrusions because of single points of failure. Acceleration Gradient (AG) is a new approach that uses the structure's surface acceleration gradient as a marker for structural anomalies. Utilizing Recent studies have demonstrated that MEMS accelerometers backed by embedded sensors boost credibility and perspective for pipeline leak detection and bridge vibration signature studies. MEMS inertial sensors based on the structural permeability detection have the advantages of miniaturization, low-cost mass manufacturing, non-invasive retrofitting, and enough redundancy to survive intrusion. CMOS MEMS, a term for the recently created monolithic manufacturing methods, has allowed accelerometers to be greatly reduced in size and cost. A capacitive combs structure is commonly used in MEMS accelerometers, It is included in

one package and coax cable to the read-out I to C (ROIC). This differs from the monolithic fabrication approach used to make CMOS microelectronics, which requires a post-processing step to add MEMS structures to a CMOS chip. As a result, an accelerometer that is small, powerful, and economical can be created. Recent studies have successfully demonstrated three-axes CMOS accelerometers with a single proof mass (SPM). In comparison to proof-mass dedicated to each axis, they are less sensitive. As depicted in the following figure:

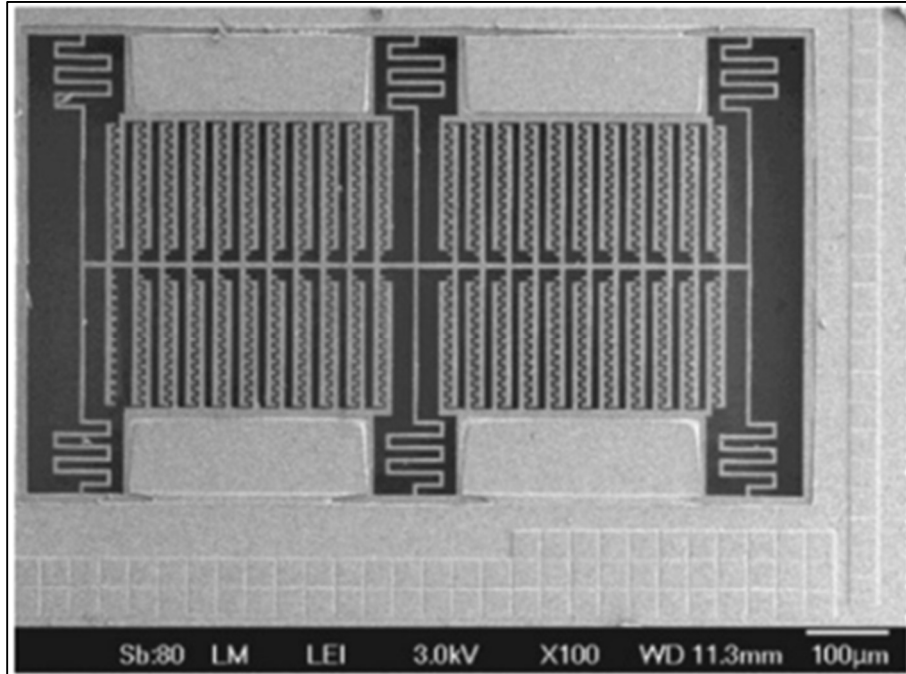


Figure 6 Microstructure of MEMS Accelerometer

#### 2.4.6 Comparison

As a consequence, many variables such as range, sensitivity, localization cost, resolution, connection, retrofitting, and servicing were used to decide the sensors' selection criterion. The most recent advancement in circuits is the integration of sensor on a single core using the CMOS technology, which gives great sensibility, range, and accuracy, as well as cost-effective, retrofittable, communication wirelessly. The following technology, on the other hand, necessitates a complex and slashing manufacturing facility, also known as an FAB house/foundry, that manufactures MEMS and CMOS electronic components. Because of the expensive cost of constructing a manufacturer, these FAB buildings are uncommon in



underdeveloped countries. On the other hand, foundries provide services to the community group while supporting the E-fabless design idea. As a result, CMOS and MEMS accelerometers and infrared imagers are commonly recognized as the ideal alternative for SHM applications where invention and characterization are unrestricted. Other sensors, such as optical fiber, SPS, an& GPRs, possess issues such as invasions, high prices and servicing, and a shortage of durability, which encourages the rise of MEMS and CMOS based sensors, such as thermal imagers and MEMS accelerometers. The following table-I qualitatively describes the above-mentioned selected strategy is highlighted:

Sensor Type	Range	Resolution	Sensitivity	Connectivity	Cost	Retrofitting	Maintenance
Ground Penetrating Radar	H	H	H	Wireless	H	Y	M
Thermal Imagers	H	M	M	Wireless/Wired	H	Y	H
Optical fiber Sensor	M	H	H	Wired	M	Y	H
Soil Properties Sensor	H	L	L	Wireless	L	Y	L
MEMS accelerometer	H	H	H	Wireless	L	Y	L

*H = High, M = Medium, L = Low, Y = Yes,*

Figure 7 SHM Sensors Comparison Plot

## 2.5 Literature Review of MEMS Accelerometer as Low Cost SHM Solution

The ever-increasing precision and ever-decreasing cost of MEMS, particularly MEMS-based accelerometers, have enabled their usage in a broad variety of industrial and scientific industries, overcoming important difficulties that were previously impossible due to device cost and size.

With in areas of seismology and seismology, the usage of MEMS acceleration sensors, that could monitor ground accelerations induced by earthquakes, has led in multiple prototypes of low-cost sensors and the subsequent creation of seismic networks solely reliant on MEMS. This has recently been characterized as as a "popular uprising in seismic detection technology," with the potential to change earthquake science due, among other things, to the cost of the sensor itself and the servicing of such a networking. 'The Quake-Catcher Network,' for example, uses MEMS accelerometer sensor designed to detect vibration at 0.1-20 Hz & accelerations generally at 2 g to operate as a strong-motion seismo station (Cochran, 2018). The Meteorological Agency of Japan 'Home Seismometer for Early Warning system of earth quake,' which incorporates a 3-hydroxy in-house MEMS accelerometer sensor capable of monitoring ground data of accelerations upto the range of 2 g at a sampling rate of 500 Hz, is another network of its kind (Horiuchi et al., 2009). 'The Taiwan's Palert Network,' for example, utilizes MEMS sensors to detect ground accelerations within 2 g at a sampling rate of 100 Hz (Wu, 2014). Acireale, Italy, pioneered the first European Urban Seismic Network (D'Alessandro, 2016), while Lefkada, Greece, pioneered local arrays of accelerographs (Karakostas Christos Z, Papanikolaou Vassilis K, 2018). It is also worth noting the research into MEMS accelerometer sensors implanted in smartphones, either as static sensor, as in the USGS experiment of earthquake and tsunami early warning deployed in Chile (Brooks, 2016) or as mobile sensors. The performance of a Raspberry-pie-based Shake 4D low-cost seismogram and acceleration sensor (Christensen, B. C., & Blanco Chia, 2017) has recently been demonstrated to be adequate for usage as just sensors in regional and local event research networks. MEMS accelerometers, as previously established, can detect earthquake-induced ground motion.

In a manner analogous to seismic waves, structural engineering is contemplating the use of sensors based on MEMs to the study of building motion. One of the most significant changes is the magnitude spectrum of the acceleration amplitudes. Using the same sensor that was mentioned before, the Communities Seismo Network (D'Alessandro, 2016) also had interfaced structures in the United States, namely in the state of California. Because of advancements in low-priced sensor technology and maintenance, dense arrays in high rise structures have been improved (Clayton et al., 2012; Zhou & Yi, 2013). The field of SHM Sensor that are dependent on accelerometers that are based on MEMS have indeed been created for the purpose of tracking sorting requirements and structure phenotypic traits, like those in bridges. Consider the following

in order to make a comparison between the peak-ground acceleration (PGA) and the acceleration of the structure's reaction. Recent earthquakes in Chile and Mexico are modeled in. Figure 9 and 8 , which illustrate the elastic frequency response with a damping factor of 5%. The response spectrum is a summary of the peak-response of the all possible linear systems with a single degree of freedom (DOF). The influence of the maximum acceleration on a range of structure system (i.e., vibration period) is significantly larger than to the PGA (like as period equal to 0) reported by strong-motion record stations. This is because the maximum acceleration has a greater impact on the structural systems. In spite of the fact that the soil type and seism genesis of the two recordings are very different from one another, it is very important to observe the ratios in between the peak-acceleration experienced by the structure system & PGA. These ratios are 5.10g and 5.31g for the recordings made in the cities of Maule and Puebla, respectively, for just a 5 percent-damped spectral response.

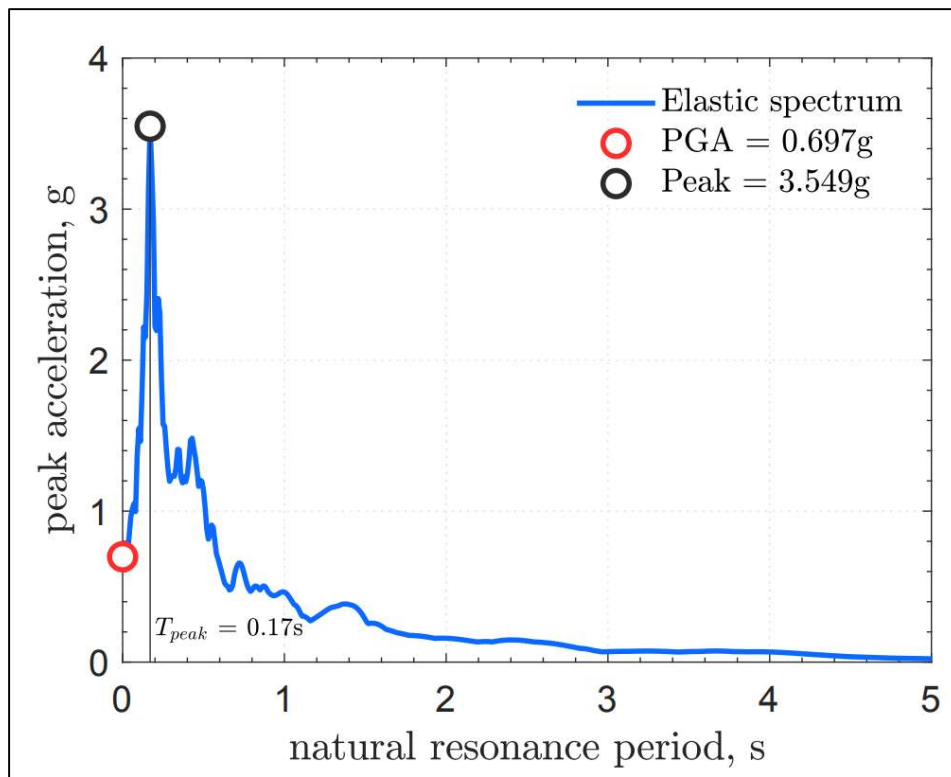


Figure 8 2010 Maule Earthquake elastic response spectrum, Channel 1, E-W, Angol station.

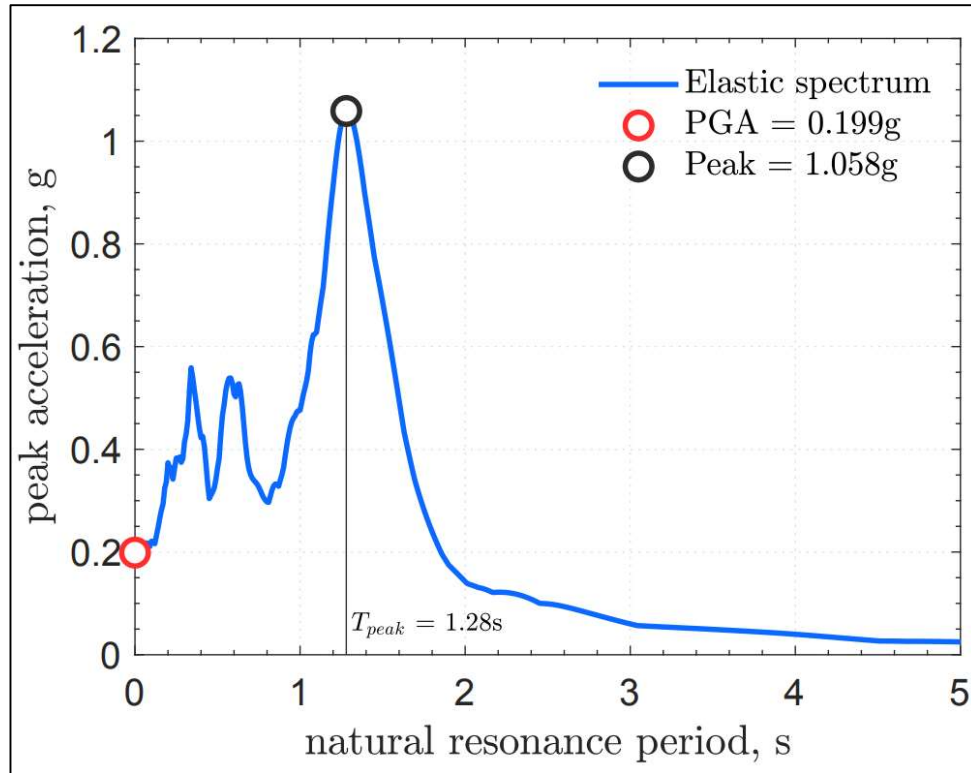


Figure 9 2017 Puebla earthquake elastic response spectrum, Channel 1, N-E, JC54 station. Both spectra have 0.05 damping.

As a consequence of this, proper evaluation of PGA has been recorded. For example, in the Maule Earthquake recording (Fig. 1a), for whom the PGA is equatable to 0.697 g, a structure may encounter a peak-acceleration of 3.549 g if the fundamental vibration period is tailored to 0.17 s. This is the case if the fundamental vibration period is tailored to 0.17 s. The clipping level, also known as the maximum range, of current strong ground motion seismic recording stations or MEMS accelerometers is often higher than this amount of acceleration. [Clipping level] [Maximum range] [Clipping level] Due to the obvious delamination that can occur within the structural system, it is common practice to use factors that affect the strength in order to lower the elastic spectrum and the design forces when designing infrastructure. This is primarily due to the fact that inelastic deformations are allowed to take place within the structural system. These accelerations grow even more in the event that there are sensitive non-str. components implanted in the floor of the structure. The roof of a multistory building can demonstrate structural reactions that are up to 18 times larger than for PGA of a single-story building. The aforementioned study examines the performance of an accelerometer that may be constructed for a minimal cost using common electrical components. In order to determine how effective a

seismograph is, for instance, it must first pass a series of tests that are based on a number of different characteristics. It is suggested that sensors might be improved in a number of ways, including through real-time monitoring, wireless networking (through technologies like Bluetooth), alternative power supply mechanisms, and routine maintenance that ensures they remain fully operational.

### EXPERIMENTAL PROGRAM

#### 3.1 Methodology

The approach of research has been explained in this chapter. Methodology includes test setup of selected sensor for stationary and non-stationary input and analysis of the MDOF structure, design for experimental setup of vibration-based sensor evaluation

##### 3.1.1 Stationary motion input

It is vital to have an understanding of the operation and design of the device in order to make use of the sensor for accurate data logging, specifically for induced accelerations. Along with batteries, cables, and aliasing caused by additional sensors, the behaviour or setup often comprises of such a MEMS accelerometers that are placed inside of a smart phone or a tiny Motherboard. Because sensors with comparable off-the-shelf electronic Modules made by the same manufacturing company may show varying performance, it is advised that individual characterization procedures be used for these sorts of sensors (Karakostas Chrstos, Papaikolaou Vassilis K, 2018). Not just for certain elements like self-noise (for example, dynamic input-based transfer functions, etc.), but also in the case of MEMS-based sensors, this variation needs to be taken into consideration in as much detail as is humanly feasible. Standardized tests are performed to characterize the overall performance of the vibration based on a micro-electromechanical accelerometer, the following is a list:

- i. Sensor noise, the purpose of testing self-noise of sensor is to establish the minimum acceleration threshold that the sensor is able to capture when operating under typical conditions.
- ii. An estimation of sensor's static sensitivity and analyzing the offset using Box flips test.
- iii. Amplitude transfer functions are constructed with inputs in the form of dynamic sine waveforms.

- iv. Integration tests, both single and double, are utilised in order to recover predominantly transitory versions of the velocity & displacement time series.

Dynamic tests were carried out with the assistance of a linear actuator after the sensing devices were coupled to the heads of a jack. In addition, a high-precision commercial accelerometer known as the LORDs accelerometer G-LINK-200 was utilised during these dynamic testing in order to get a specific interaction of the actuator's output waveform. This is an essential standard procedure whereby, in addition to examining the exact behaviour of a mechanical means utilised in the trials, helps in detecting alternate sources of varying load noise. In other words, it does both of those things simultaneously. As will be discussed further down, the linear actuator that was utilised in the tests was found to be the source of some mechanical noise and perhaps some spurious behaviour in the locked feedback system. This behaviour manifested itself most noticeably at the maxima of the sine wave when large amounts of generated acceleration were present. As a consequence of this, the linear actuator was able to reach an effective frequency of 17 Hz for sine waves with low amplitudes. This frequency represents the maximum frequency that was tested throughout the process of the construction of the sensor's intensity transfer functions. In order to evaluate how the proposed system would react, a set of dynamic tests are performed on two mockups that are virtually identical to one another in terms of their electronic design (i.e., standard test 4 and 3).

### **3.1.2 Non-stationary motion input**

Collection of Non-Stationary Strong motion record is used in a shake table to perform dynamic analysis, which is then measured either by prototyped accelerometer or the typical commercial sensor discussed earlier. The chosen record were based on variety of some core characteristics, including PGA, peak-acceleration, time duration, and dynamic energy contents. The collection of records has been divided into three categories for the purpose of making the results more easily interpretable: simple sine wave form, seismic wave form, and mode shape. A detailed description of the character traits of the recordings is discussed later, and The analysed qualitative and quantitative results may be seen below; these results were derived from the recorded data:

- i. It is determined how accurate the raw recorded acceleration signal is, in addition to the displacement and velocity signals that are acquired by incorporating the processed acceleration record.

- ii. Error in computing the Fast Fourier-Amplitude Spectrum (FAS).
- iii. Structure dynamic response data reliability, robustness, and bias.

### 3.2 Model Description

A prototype 3-D steel frame is developed having 4 storeys. Each storey is 18” tall. Each storey's beam measures 23.5” in length. Table 3.1 shows the primary dimensions of the elements of the structure. And Table 3.2 list the fundamental structure's additional properties, such as mass, stiffness, and damping

Table 1 Description of Model

	Length	Thickness	Diameter
Column	18”	--	1/4”
Beams	23.5”	--	3/16”
Diaphragm	23.5”x23.5”	16 Gauge/ 0.06” (1.5mm)	--

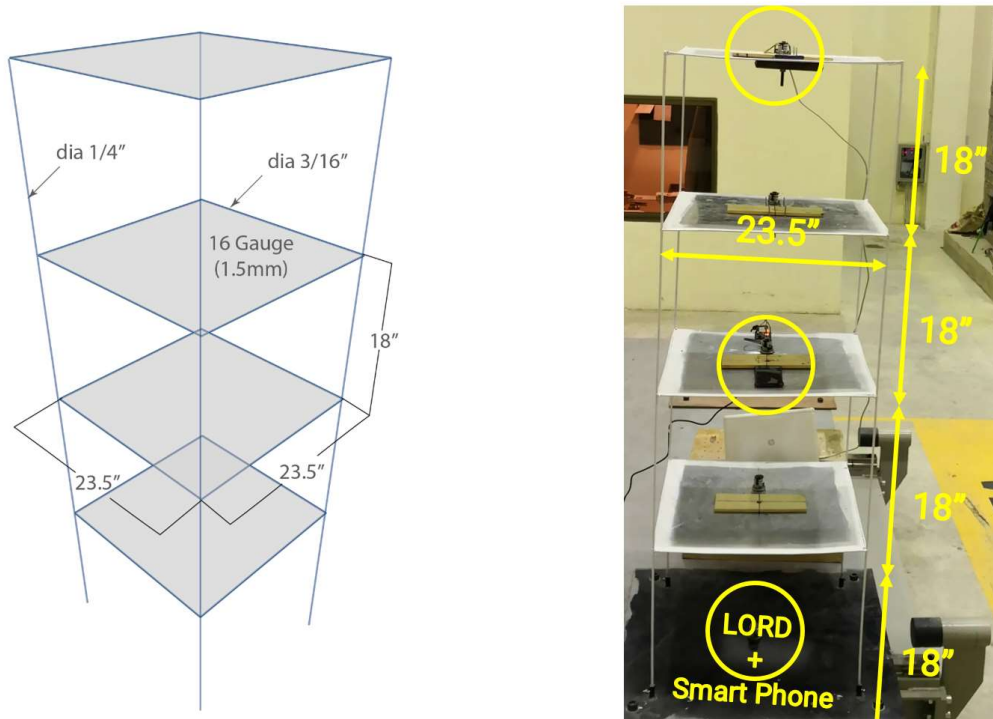


Figure 10 Experimental & Schematic Model of Structure'



Table 2 Structure Primary Parameter

Storey level	Mass (Kg)	Stiffness (N/m)	Damping (Nsec/m)	Natural Frequency (rad/sec)
1	9.98	8017	7.238	9.8434
2	9.98	8017	7.238	28.3428
3	9.98	8017	7.238	43.4238
4	9.98	8017	7.238	53.2671

### 3.3 Sensors Parameters

#### 3.3.1 LORDs Accelerometer (G-LINK-200)

The G-Link-200 is a wireless 3-axis accelerometer with a durable, waterproof casing that runs on batteries. This wireless accelerometer is ideal for monitoring the dynamic characteristics of structures experiencing seismic loading. The G-Link-200 delivers exceptionally low noise waveform data, making it excellent for applications such as vibration, impact, and motion monitoring. It uses three LiSOCL2 batteries and has a base made of stainless steel.



Figure 11 G-Link-200 Wireless Triaxial Accelerometers - LORD Microstrain

Table 3 G-Link-200 Wireless Triaxial Accelerometers - LORD Microstrain Parameter

<u>Specification</u>	<u>Design value</u>
Max Nominal acceleration	$\pm 2$ to $\pm 40$ (g)

Baurd rate for Y & X axis	DC to 1K (Hz)
Bandwidth for Z axis X	DC to 1K (Hz)
Acceleration delicacy	300 m V/g $\pm$ 30
X and Y axis Noise Density	25 $\mu$ g/ $\sqrt$ Hz to 80 $\mu$ g/ $\sqrt$ Hz
Z axis Noise Density	25 $\mu$ g/ $\sqrt$ Hz to 80 $\mu$ g/ $\sqrt$ Hz
Sample rate	1 sample/Hr to 4096 Hz

**3.3.2 BMI160 IMU combining accelerometer and gyroscope**

The BMI160 is a small, low-power 16-bit IMU especially designed for Smart Phone applications such as Augmented reality technology or indoor navigation, offering highly accurate sensor information as well as real-time sensor data. BMI160's low current consumption enables everytime applications in battery-powered devices. This sensor features a configurable on-chip interrupt engine which provides motion-based gesture recognition and context awareness as always-on background functions. The BMI160 is compatible with the Qeexo FingerSense application.

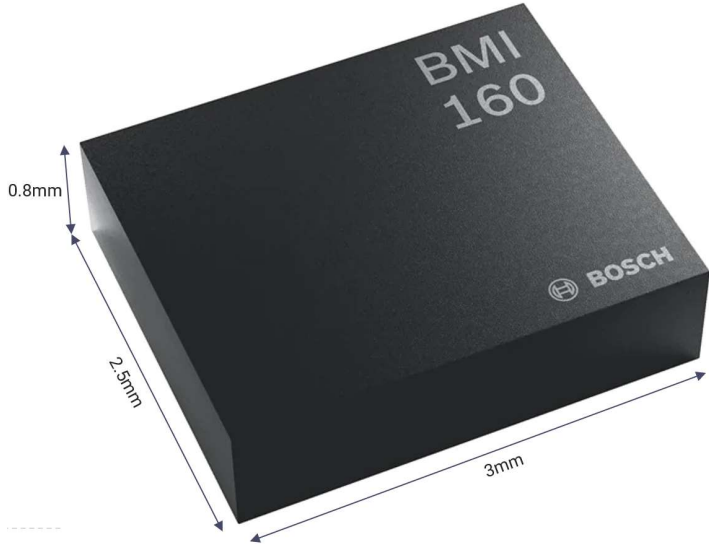


Figure 12 BMI160 IMU combining accelerometer and gyroscope schematic

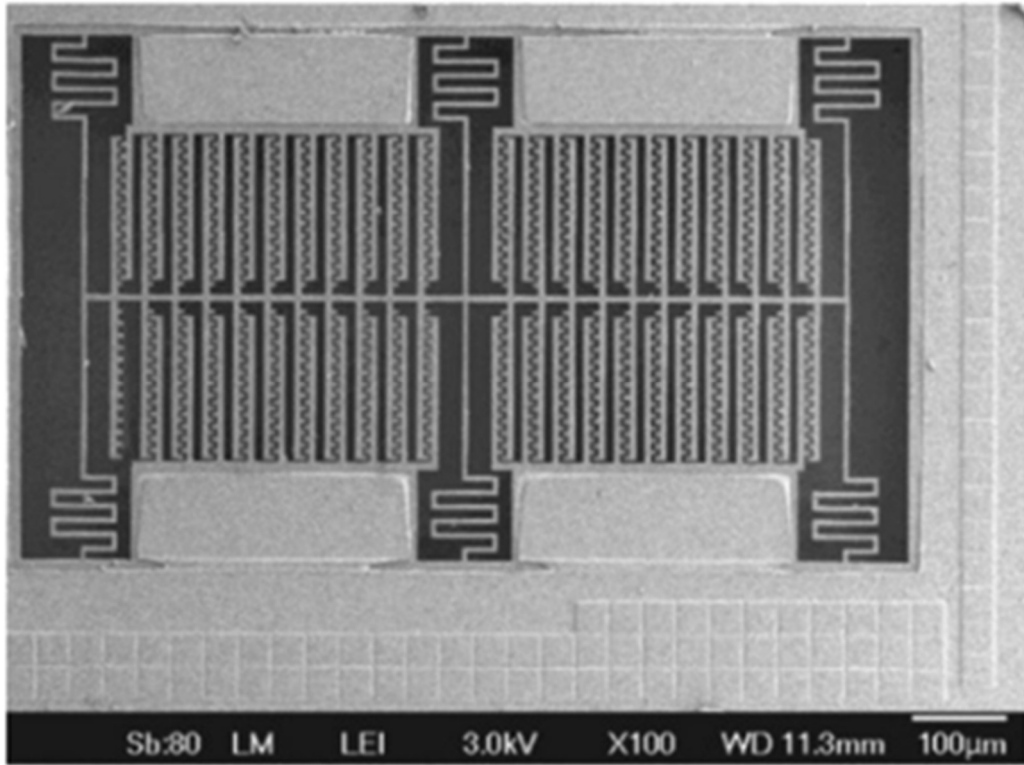


Figure 13 Microstructure of MEMS Accelerometer

Table 4 BMI160 IMU Combining Accelerometer and Gyroscope Parameter

<u>Specification</u>	<u>Design value</u>
Max Design Acceleration	$\pm 2 \text{ g to } \pm 16 \text{ (g)}$
Baud Rate for X and Y axis	1600 (Hz)
Baud Rate for Z axis X	1600 (Hz)
Acceleration delicacy	$300 \text{ m V/g } \pm 30$
X and Y axis Noise Density	$150 \mu \text{ g}/\sqrt{\text{Hz}} \sqrt{\text{rms}}$
Z axis Noise Density	$300 \mu \text{ g}/\sqrt{\text{Hz}} \sqrt{\text{rms}}$
Sensor Resonant Frequency	5.5 kHz

### 3.4 Testing Platform

The shake table used in this research experimentation is manufactured by BESMAK and has a platform of 4m x 4m with a max payload capacity of 12 tons. The platform moves with the help of a single ended servo hydraulic actuator. Displacement capacity is 350mm from the center and supports acceleration up to 2g.



Figure 14 BESMAK Shake Table Platform

#### 3.4.1 Actuator

The shake table uses actuator manufactured by BESMAK. It is a single-ended servo hydraulic actuator. Servo Hydraulic Actuators provide an integrated, high-performance solution our dynamic force generation requirements. The actuator act as linear or variable displacement transducer. Two hydraulic motors (as shown in Figure) power the actuator to produce displacement in the platform simulating earthquake.



Figure 15 BESMAK Dynamic Actuator

### 3.4.2 DOLI Data Acquisition System

EDC controllers are imported from Germany and are commonly used for machine testing with high confidence or requirements. The EDC220 is a built-in device for static and dynamic testing equipment that lacks keys and a display. It has steady control, high accuracy measurement, and a high sampling rate (1 kHz-5 kHz), among other advantages. It also has self-identification and self-calibration capabilities. Until date, it has been the most dependable device for both static and dynamic testing machines.

On-board are all the measurement channels for a simple testing equipment, as well as an output channel for controlling an actuator. Extensometers, for example, can be connected to the EDC220V's two I2-Bus-Extension-Slots. The EDC220V's inbuilt load channel has a resolution of 180,000 step



Figure 16 DOLI Data Acquisition Controller

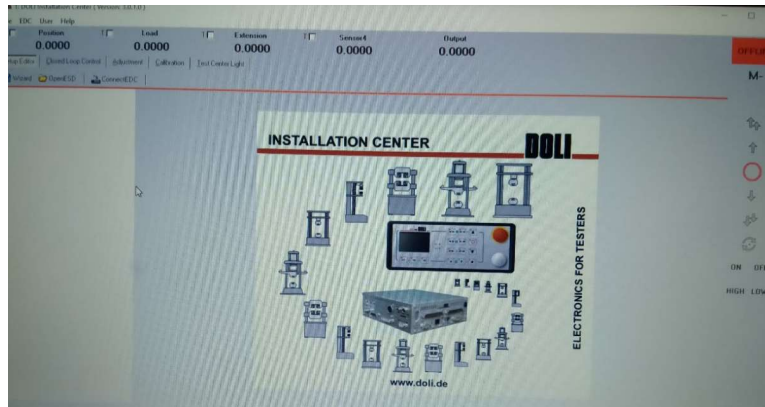


Figure 17 IDE for DOLI Control System

### 3.4.3 Hydraulic Valve

The hydraulic valve is used to control the flow of hydraulic fluid which in turn extend the arm of the actuator. The hydraulic valve used in our experimentation was manufactured by Parker. Parker Hannifin has a leading technology in the hydraulic market: the DFplus® range of proportional directional control valves. The outstanding performance of the revolutionary Voice Coil Drive VCD® is comparable to that of servo valves. DFplus can reduce the initial and ongoing expenses of high-end hydraulic systems and ordinary applications



Figure 18 Servo Valve

### 3.4.4 Node MCU

The BMI 160 can be installed using a variety of control boards. One of the most notable control boards in the ground is Node-MCU. First, as shown in Figure 20 Schematic Diagram. the cables must attach the deck to the accelerometer. The USB is then connected to the computer, completing the circuit. Using the code presented in the IDE image, we can now access the connection apps from the manufacturer's website. This code has been loaded onto the board. Acceleration data are garnered in x, y, and z di- reactions in the Serial Monitor. BMI 160 exhibits x-y-z direction alignments.

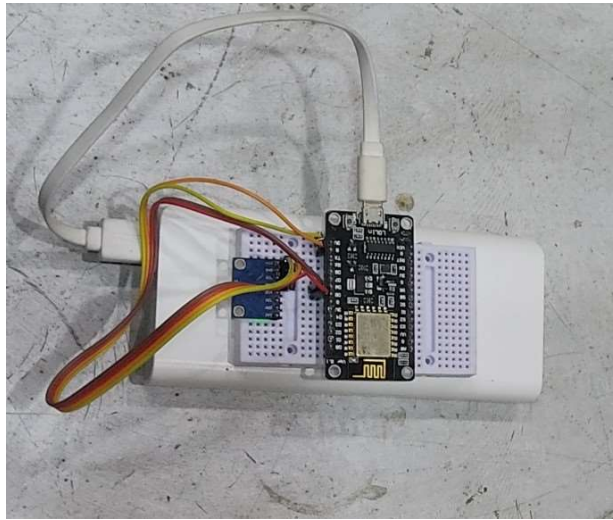


Figure 19 Microcontroller base Experimental Setup of BMI 160

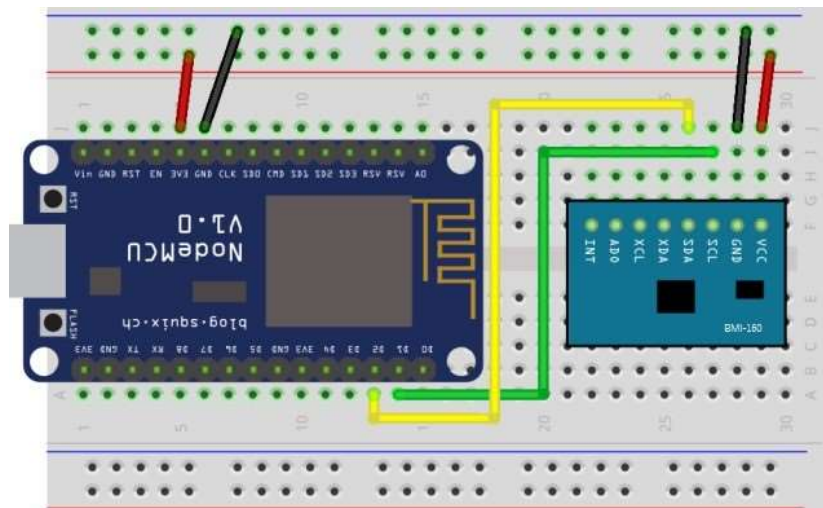
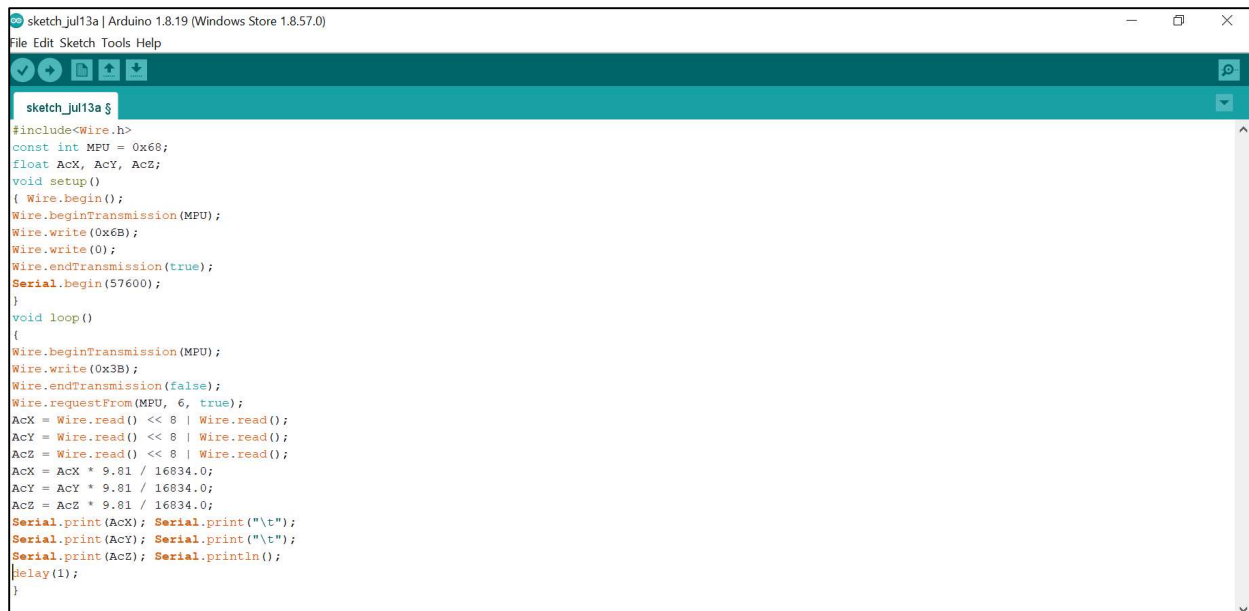


Figure 20 Schematic Diagram





The screenshot shows the Arduino IDE interface with a sketch named 'sketch\_jul13a'. The code is as follows:

```
sketch_jul13a $
#include<Wire.h>
const int MPU = 0x68;
float AcX, AcY, AcZ;
void setup()
{
  Wire.begin();
  Wire.beginTransmission(MPU);
  Wire.write(0x6B);
  Wire.write(0);
  Wire.endTransmission(true);
  Serial.begin(57600);
}
void loop()
{
  Wire.beginTransmission(MPU);
  Wire.write(0x3B);
  Wire.endTransmission(false);
  Wire.requestFrom(MPU, 6, true);
  AcX = Wire.read() << 8 | Wire.read();
  AcY = Wire.read() << 8 | Wire.read();
  AcZ = Wire.read() << 8 | Wire.read();
  AcX = AcX * 9.81 / 16834.0;
  AcY = AcY * 9.81 / 16834.0;
  AcZ = AcZ * 9.81 / 16834.0;
  Serial.print(AcX); Serial.print("\t");
  Serial.print(AcY); Serial.print("\t");
  Serial.print(AcZ); Serial.println();
  delay(1);
}
```

Figure 21 IDE Node MCU Sketch

```
#include<Wire.h>
const int MPU = 0x68;
float AcX, AcY, AcZ;
void setup() {
  Wire.begin();
  Wire.beginTransmission(MPU);
  Wire.write(0x6B);
  Wire.write(0);
  Wire.endTransmission(true);
  Serial.begin(57600);
}
void loop() {
  Wire.beginTransmission(MPU);
  Wire.write(0x3B);
  Wire.endTransmission(false);
  Wire.requestFrom(MPU, 6, true);
  AcX = Wire.read() << 8 | Wire.read();
  AcY = Wire.read() << 8 | Wire.read();
  AcZ = Wire.read() << 8 | Wire.read();
  AcX = AcX * 9.81 / 16834.0;
  AcY = AcY * 9.81 / 16834.0;
  AcZ = AcZ * 9.81 / 16834.0;
  Serial.print(AcX);
  Serial.print("\t");
  Serial.print(AcY);
  Serial.print("\t");
  Serial.print(AcZ);
  Serial.println();
  delay(1);
}
```

Acceleration Data Collection Code



## RESULTS AND DISCUSSIONS

### 4.1 Introduction

This chapter summarizes and analyses the results of tests done on Prototype Module, including the evaluation of MEMS accelerometer for vibration base Structural health monitoring Under standard laboratory testing procedure. The prototype accelerometer sensors used to collect data for stationary and non-stationary input motion and output signals were analyzed for sensitivity, noise and behavior under seismic excitation.

### 4.2 Prototyped sensor's general performance

#### 4.2.1 Self-noise of sensor

Since sensors produce noise, it is possible to estimate the device's weakest detectable movement (Rodgers, 1992). A sensor's self-noise can be measured in a number of ways, but the Power Spectral Density method (PSD) was chosen for this study. According to Equation 1. The PSD is expressly defined as follows:

Equation 1

$$S_{xx} = \int_{-\infty}^{\infty} R_{xx}(\tau) e^{-i\omega\tau}$$

The autocorrelation function for the signal is represented by  $R_{xx}$ , and its two-sided PSD is represented by  $S_{xx}$ . As shown in Figure 22 - 12 h Continuous Recording for Noise Test, we were able to determine the MEMs accelerometer's frequency-dependent self-noise by looking at the Power Spectral Density of the data acquired by our system over a period of 12 hours.

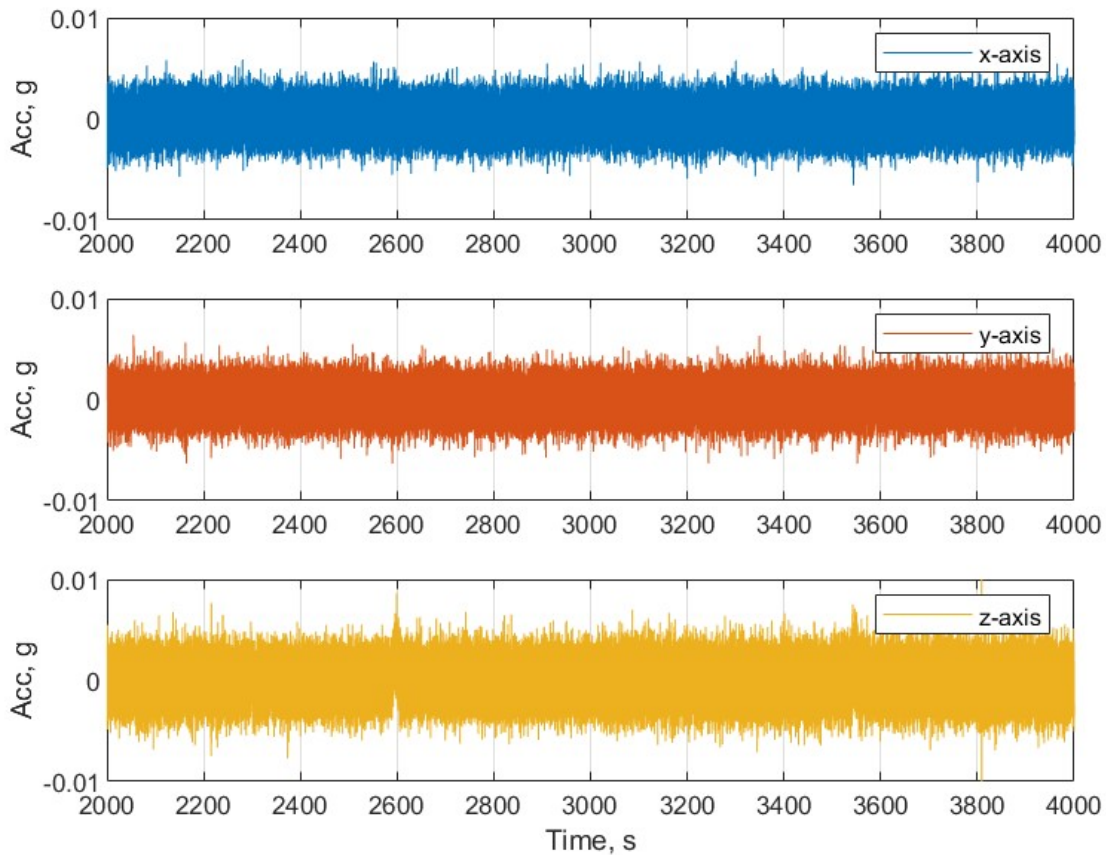


Figure 22 - 12 h Continuous Recording for Noise Test

The low Power spectral density of an incidental ground shaking signal was assumed to be sufficient to describe the overall low-cost system. And it can be used to record strong-motion accelerations. On the basis of data from sensor 1, the PSD curves for acceleration are shown in Figure 23 - Average PSD of MEMS accelerometer data over 12 hours of idle state. The Welch method (Welch, 1967) was used to calculate these, with 32-Hanning windows & 50% overlap set based on tests within each of them. The response and shape of the three axes are remarkably consistent over a wide frequency range. For low frequency, Z-axis demonstrates a 3 to 4 times considerably greater value of acceleration PSD than concurrent behavior of Y & X-axis, but this trend holds true for the frequency range of above about 1.0 Hz. The manufacturer's typical standards for RMS noise are shown in Table 4 BMI160 IMU Combining Accelerometer and Gyroscope Parameter. The three axes exhibit low self-noise PSD (i.e., strong signal/noise ratio) for signals generated by mild earthquakes in the relevant frequency range for earthquake

engineering (0.2-20 s), allowing for signal capture (Clinton & Heaton, 2002; D’Alessandro et al., 2017). The smoothed values depicted in Fig. 5 were calculated that used 20-point and 10-point mean vibrant algorithm, respectively, for hz below and above 1.0.

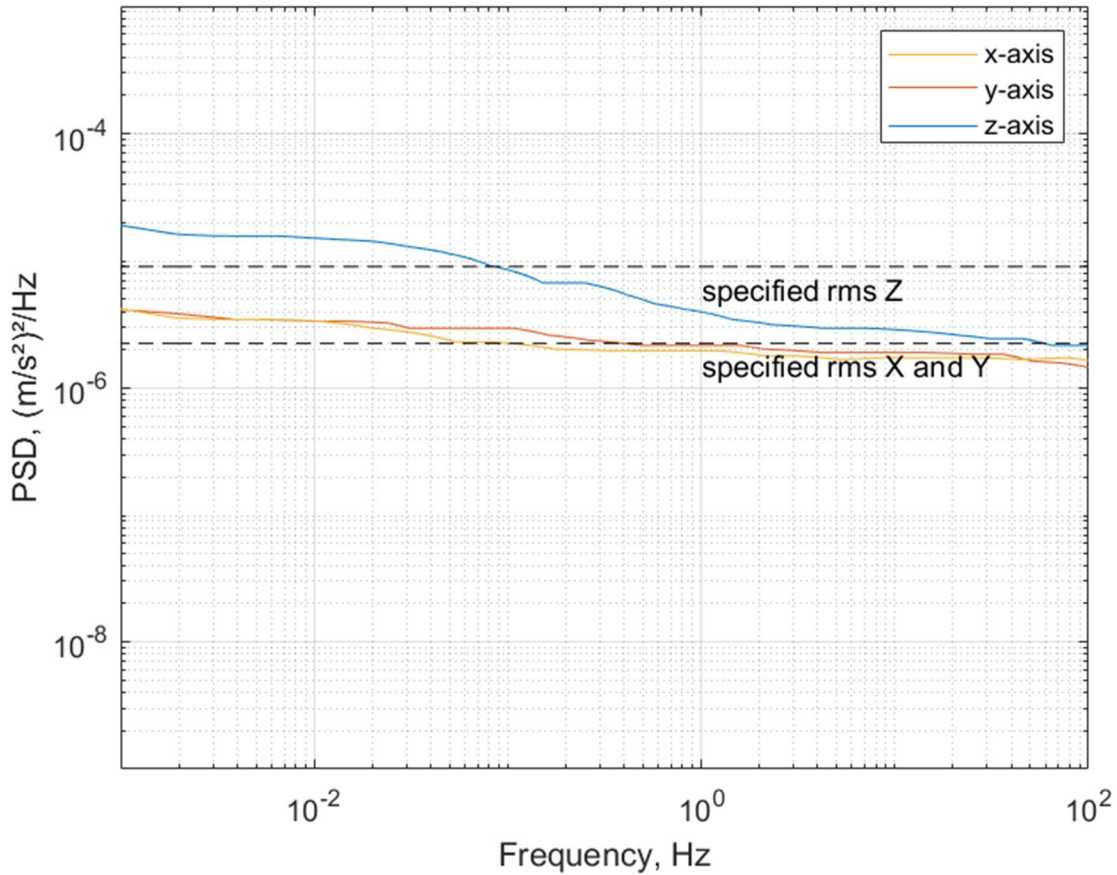


Figure 23 - Average PSD of MEMS accelerometer data over 12 hours of idle state.

By average out the time dependent signal data  $x(t)$  over a window of time, the possible deflections or drifting were also estimated using the 12 h samples. Each axis' 12-hour average is  $0.181 \text{ m/s}^2$ ,  $0.118 \text{ m/s}^2$ , and  $0.088 \text{ m/s}^2$  (1xg).  $1.440 \times 10^{-3} \text{ m/s}^2$ ,  $2.847 \times 10^{-3} \text{ m/s}^2$ , and  $3.088 \times 10^{-3} \text{ m/s}^2$  stand. variation per axis. In order to fine-tune the sensor, the average measured across all axes must be removed or detrended because there are no unique patterns or time-dependently rising average values. The maximum acceleration of the input signal was 0.06 g. For a

statistically precise evaluation of the sensor's dependability and variability, additional ego test results on several sensors are required.

#### 4.2.2 Flip Box tests

The sensor offset, axis alignment, and stationary (0 Hz) sensitivities were assessed using a box-flip test. The MEMS accelerometer can fit inside a cubic box because its axis is parallel to the boundaries of the container. The container can be rotated thru the 6 possible positions using the gravitational acceleration as a guide with all axis in the downhill and upward orientation. This technique can be used to calculate the stationary sensitivities of each axis and the possible accumulation of drifts when the box is in its initial location. Evans et al. (2014) The Earth's static field is frequently used as a relation to roughly estimate the discrepancy in between sensor's values and those reported by the sensor (e.g., when employing an ultimate gravimeter). As a result, the test is repeated ten more times to assess the variance of the recorded values. The recorded values are then compared with standard value of 9.806 m/s<sup>2</sup>, which is unavailable here.

An example of a box-flip test based on BMI-160 results can be seen in Figure 24 Sensor data flip-box test. The top plot shows the sensor's positions during the test; The axis's either upward downward positions in relation to a level ground are indicated by the arrow. In the top plot, the sensor's orientation is shown sequentially from right to left for a static position. The transient motion of the box causes the signal to be perturbed between the two fixed positions. The sensor's sensitivity and variability were calculated using a median of the value observed during the nil window, which was defined by the dashed vertical stripes. At the end, there are only very slight variations from the initial measurement taken at the start of the test. Double-integration of the acc. recording is essential for retrieving accurate displacements with the former.

The calibration curve's slope shows the calculated static sensitivity, which is 316.36 mV/g on average across the three axes. This value is very close to the manufacturer's stated typical sensitivity of  $3 \times 10^{-4} \text{ V/g} \pm 3 \times 10^{-5}$ . Value was computed straight from the raw data gathered during the zero-movement window of the box-flip test. Low-cost, commercially accessible MEMS accelerometers are getting more and more accurate compared to recently published static sensitivity values. (Evans et al., 2014a)

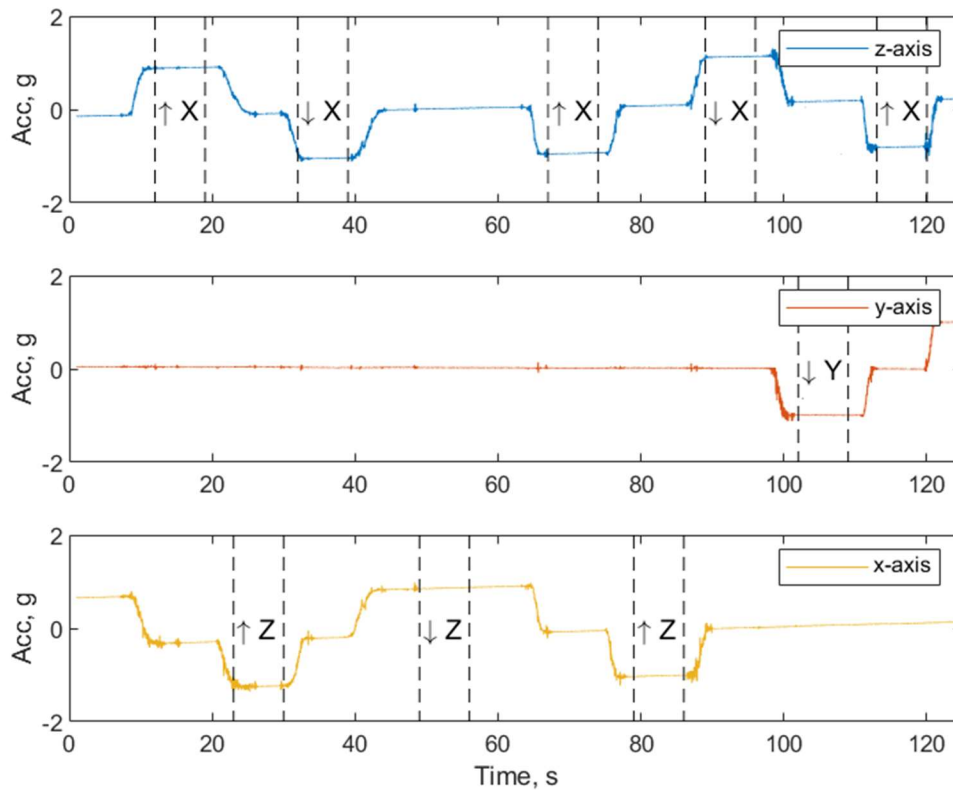


Figure 24 Sensor data flip-box test. The top plot shows the sensor's positions during the test; The axis's either upward downward positions in relation to a level ground are indicated by the arrow.

### 4.2.3 Transfer function tests

The transfer function of a system is the proportion of output to input. For instance, it is possible to correlate the signal sent to a dynamic jacks input with the magnitude and frequency of a sensor's data signal. The emphasis is on measuring the magnitude response ratio for a wide variety of signals at various frequencies in order to estimate the sensor's "flat-response" range. The transducers and MEMS sensors gathered all the information sinusoidal waves with different amplitudes and frequencies to use a uniaxial fluid actuator. The fluid actuator control system receives an ideal synthetic signal, but because the jack performs significantly differently in practise, the elevated transducers data is used as a reference in the analyses that follow.

A RMS value of the acceleration record can be used to calculate amplitude ratios directly in the time domain, or a spectral analysis can be used to do it in the frequency domain. As a result, the

sensing element's RMS sensitivities to noise from multiple sources (Evans et al., 2014a) is main disadvantage for the former. The actuator stroke must be as long as possible in order to achieve the lowest possible level of vibrations in terms of acceleration, especially for low-frequency weak signals. This eliminates both the external and internal noise. Particularly when dealing with low-frequency weak signals that necessitate the longest actuator stroke possible in order to achieve the lowest possible level of acceleration excitation, internally and externally noise can be overcome. To determine the net power of the signal's dominant frequencies, we use the method described in (Evans et al., 2014a) . Figure 25 Raw data from a 4 mm, 4 Hz sinusoidal input signal. and Figure 26 Raw data from a 4 mm, 4 Hz sinusoidal input signal. show this for a sinusoidal input with design amplitude & frequency 4 mm & 4 Hz, respectively.

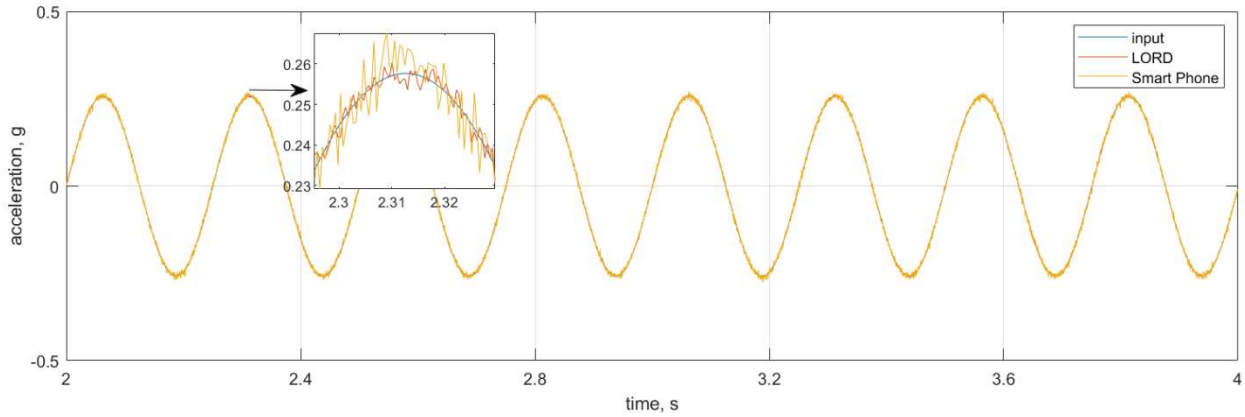


Figure 25 Raw data from a 4 mm, 4 Hz sinusoidal input signal.

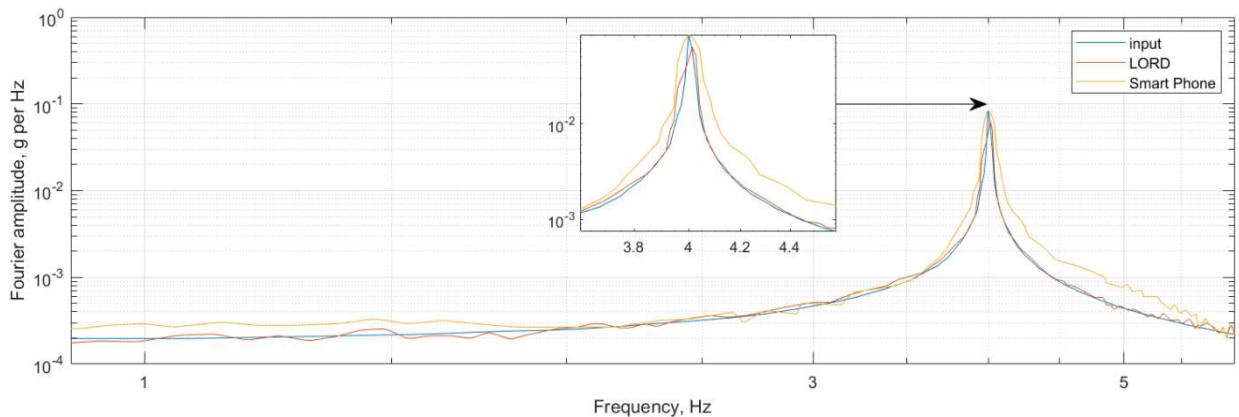


Figure 26 Raw data from a 4 mm, 4 Hz sinusoidal input signal.

Figure 25 Raw data from a 4 mm, 4 Hz sinusoidal input signal. shows a snippet of the evaluated signal data by the accelerometers & transducer, along with synthesised input data, whose response spectrum shown in Figure 26 Raw data from a 4 mm, 4 Hz sinusoidal input signal. spectral analysis. Using a slender band of frequencies close to the main frequency's peak, whose value for sensors is usually reference input frequency, noise can be removed from the signal by filtering out frequencies outside of this band. An acceleration value is generated by calculating the root-mean square of the FFT amplitudes of the five frequency points from around sensor's reported peak amplitudes.

As an aside, first, let's talk about the intensity ratios of all sine wave input signals, it is important to note that the sensor's sampling rate is fixed at 512 samples per second, whereas the transmitter is sampling at rate of 2048 samples/second, given the DAQ system's ability. In Figure 26 Raw data from a 4 mm, 4 Hz sinusoidal input signal. an accurate match of the synthesised sinusoidal waveform input to the oscillator is achieved by using the original data of the transducer. Figure 28 Amplitude ratio of LORD signalsshow amplitude frequency response for MEMS accelerometers, This can be calculated using the linear actuator's input signals' spectrum evaluations. In particular, 24 sine-wave cycles were taken into account. The amplitude ratio suggests positive actions given the homogeneity of the amplitudes for input signal, which was constrained by the dynamic equilibrium of a servo.

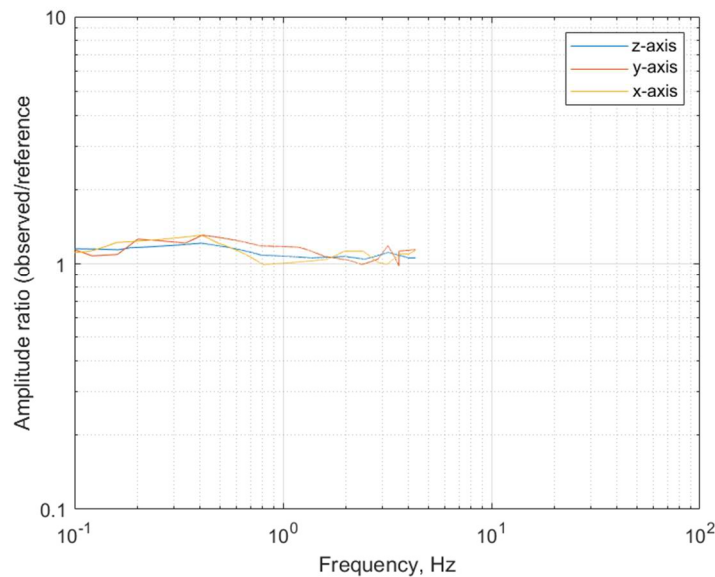


Figure 27 Amplitude ratio of Smart phone

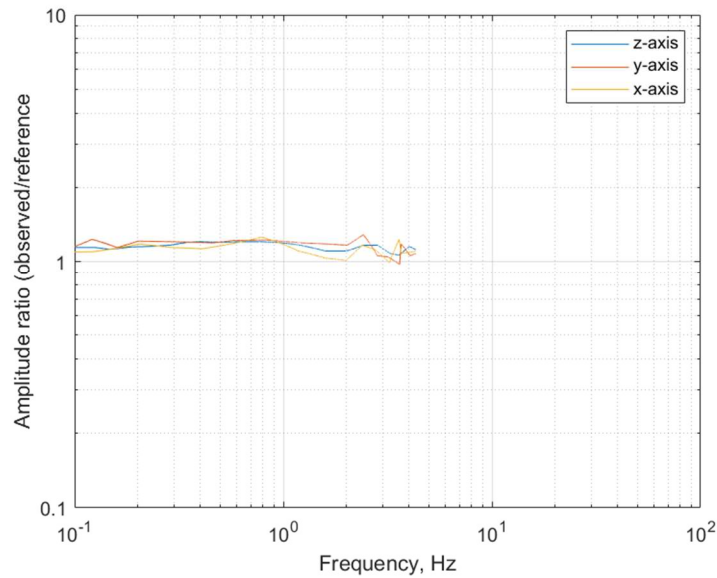


Figure 28 Amplitude ratio of LORD signals

#### 4.2.4 Sensor linearity and Clipping behavior

The linearity means that the output and input signals have a linear relationship (Evans et al., 2014b). To determine the degree of sensor linearity, it is common practise to perform calculations using a fix frequency and varying amplitudes. According to (Evans et al., 2014b) a linearity of 1% is considered acceptable for sensors intended to assess strong ground motion. Comparing sensors is made more difficult by the fact that linearity levels are rarely specified. Once any threshold is crossed, compared to the input signal, the captured signal is distorted. When using accelerometers, the mechanical ability of the sensor is commonly used as a threshold, which is approximately  $\pm 1$  g for BMI-160. Sensor behaviour can vary widely, especially with MEMS accelerometer, as studied by (Evans et al., 2014a) where a few devices alter the recorded signal rather than clipping it. It's better to just blow it up and get rid of it entirely. When using double integration to extract the displacement requirement from the revealed acceleration signal, the latter type of inappropriate clipping actions is undesirable because it could limit the sensor's capabilities.



In order to evaluate linearity and clipping, input sinusoidal waveform inputs are converted into the servo, and response amplitudes are estimated using spectral analysis as was mentioned in the preceding section. With the input fixed frequency at 4 Hz, which is small in the region of interest, a varied magnitude is employed to create a range of acceleration between 0.2 g to 1 g. In contrast to the output signal recorded by the transducer, Fig. 10 shows the seamless clipping action of BMI-160 for uniform accelerations all around the nominal clipping layer of a MEMS accelerometer. In Figure 25 Raw data from a 4 mm, 4 Hz sinusoidal input signal., However, as acceleration rises, transducer output signals also increase. LORD observed a clean clipping pattern as well. Figure 27 Amplitude ratio of Smart phone the amplitude ratio vs. acceleration levels using the amplitude ratios obtained using the spectral approach. According to (Evans et al., 2014a), the RMS output for a sine wave is typically calculated as the absorption of the 3 axes of the sensors clip given their mild attenuation above their normal clip cutoff, which is represented in the plot by a vertical dashed line.

#### **4.2.5 Double & Single integration test**

Monitoring a structure or structural system necessitates the ability to extract both long-term and short-term displacements from acceleration data. These ratios are generally the most important in earthquake engineering because they can be easily linked with damage states, which are typically predefined by structural configurations of the system (Bravo-Haro & Elghazouli, 2018). When estimating structural losses and making decisions about whether or not to demolish or retrofit a building after a disaster, residual or perpetual drifts deserve special consideration because of their critical role in reply assessment (Macrae & Kawashima, 1997). In order to extract velocity and displacement time historical events from acceleration recordings, the double and single integration processes are commonly used, respectively. Although the displacement and velocity have nonphysical waveforms, this is an unsolved problem (Evans et al., 2014b). There are a number of potential error contributors, including: baseline offset, noise cancellation, and artefacts due to velocity and displacement measurements not knowing their initial circumstances., all contribute to these erroneous results (Boore, 2005; Boore & Bommer, 2005) It has been suggested that these errors can be remedied by employing a variety of methods including various baseline adjustments, filtering and zero-padded sections.

Same as previous section dynamic tests with sine wave input signals are used here. These tests also weren't designed to generate residual deformations that can be recovered later, so the main goal here is to measure displacement and velocity transient wave patterns through time-histories. Based on the accelerometer record, a cube polynomial function was fitted that is then subtracted from a recorded acceleration to create a baseline correction. For the first time, there are no padded sections at the beginning or end of the record, which is based on the sequence & corner frequency for filtration also be adapted afterward. A 3-order Butterworth bandpass filter with cornering filtration frequencies of 25 Hz & 0.1 Hz is used to further reduce noise. Lower limits were chosen to reflect pretty standard limits of long-term structures, while upper bounds were set in accordance with mechanical noise seen in actuator signal data.. The displacement and velocity time histories are then computed by numerically integrating the acceleration data. Transducer data was used in the same way as actuator data to make comparisons based on actual actuator output. A sine wave input signal with different nominal frequency and amplitude is applied to two different single and the double integration procedures, as shown below:

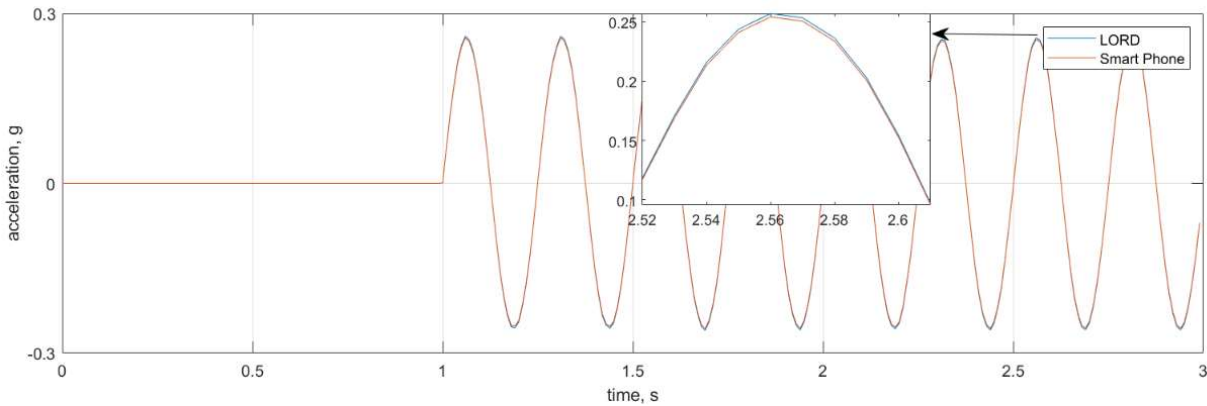


Figure 29 Sinusoidal wave Acceleration plot

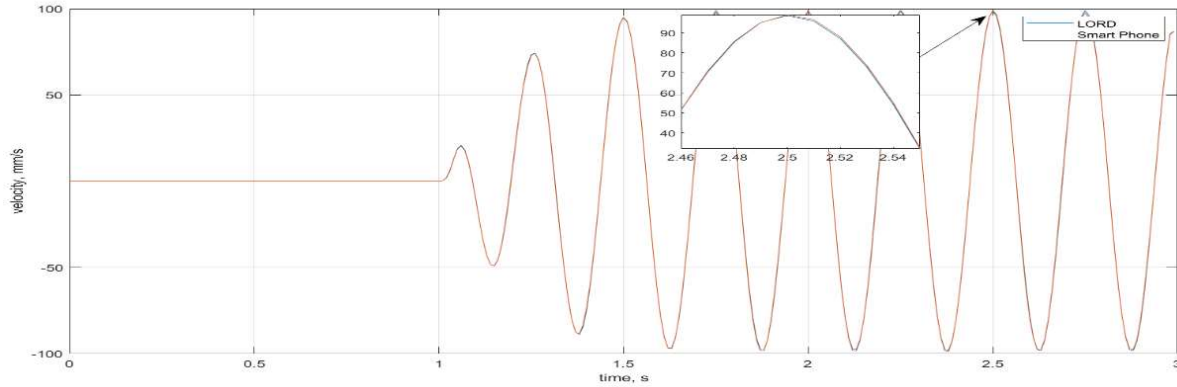


Figure 30 Sinusoidal Wave Velocity plot

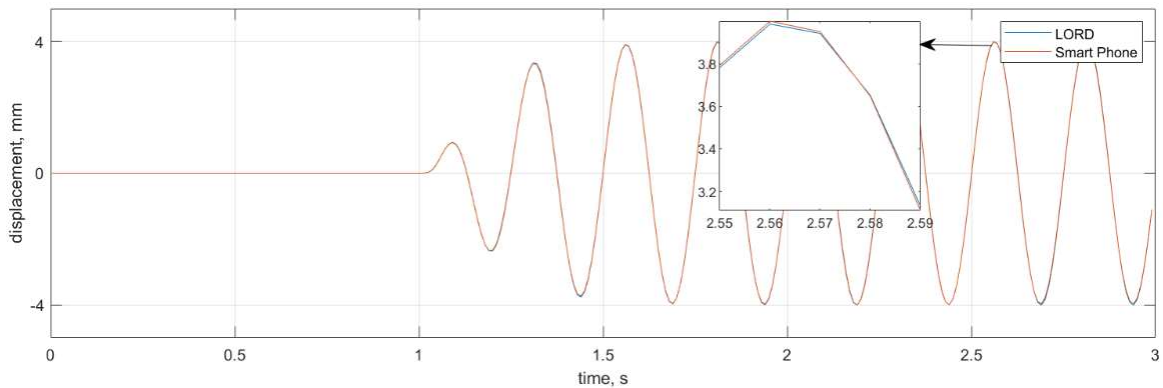


Figure 31 Sinusoidal wave displacement plot

In general, the sensor does a good job of recovering step amplitudes and waveforms, which is critical at this early stage because of the stable sampling rate. This non-steady behaviour can be seen in both displacement time-histories that were recovered, before they reach their steady states. At first, it was thought that the transducer's peculiar behaviour was due to the noise removal; however, the sensor continuously managed to capture it even when various process methods were used before the assimilation of the signal (including zero-padded regions lengths and other filters like Chebyshev). In addition, there was repeatable behaviour in the initial oscillator control, especially at the tested peak locations. Please remember that low-cut filters cannot be used to recover residual displacement by double-integrating the acceleration data (Evans et al., 2014a), thus, independent measurements of negates or residue left deformations in

the servo response of structural components are preferable when evaluating the sensor. Figure 31 Sinusoidal wave displacement plot.

### 4.3 The prototype seismic sensor's performance.

Information was gathered by simulating earthquakes with a shake table, and the outcomes are discussed here. The signal from the LORD, or reference, sensor was recorded at 1024 sps, while the BMI-160 was sampled at 512 sps to conform to the specifications of the data acquisition system. Consequently, we had to subsampling the acceleration data recorded by the source device using the Matlab function "decimate," which delivers the same result when tuned properly, and "downsample," which achieves the same results with control methods. It's important to note that decimation employs a low-pass filter implemented as a FIR filter before resampling the signal at a lower frequency ( $x = 4$  here). The decimate function was used, with the filter order set to 3.

### 4.4 Input and response parameters

Important features of seismic data used in shaking table testing are described below. Figure 32 Earth quack input to the systeme arth quack of 0.2715 g PGA was used on shake table having unique frequency band it is the seismic wave formation having RMS value of 0.0182. This is use as non stationary standadize input evaluation testing. Here we will check system for Accraicy acesment of signals using singel and double itegration method, efficiency of FAS fourier amplitude spectrum which wil help to observe static sensitivity of sensor and in last determined the real time Dynamic response of structure, how efficiently sensor can capture it.

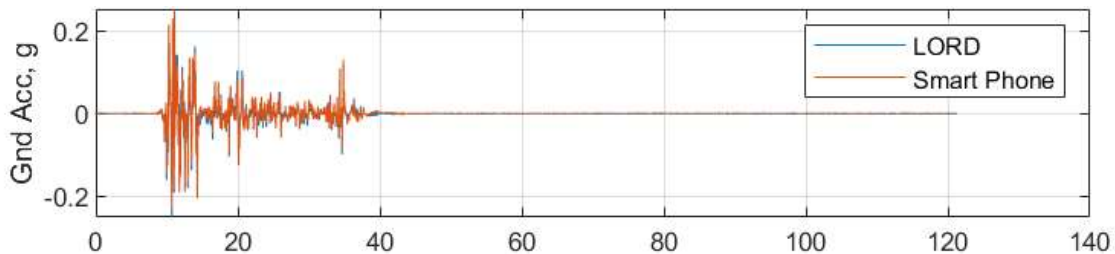


Figure 32 Earth quack input to the system

## 4.5 Accuracy Assessment Raw Signal

There were two sensors attached to the shake table, one on each side, that recorded time-acceleration data, which was processed as described in the previous section. Figure 33 Story wise acceleration dataa single far-field record and a single relatively close record, respectively, are evidenced in regards to FAS, acceleration, velocity and displacement. Several techniques were tried before settling on the pass method for synchronising the waveforms. In order to compute the correlation (maximum equal to 1.0) between the signals, this allows the computation of the signal's time-lag vs. the time-lag vectors, resulting in time-lag correlating to the biggest correlation. According to the waveforms, PG values of acceleration, velocity, and displacement for reference signal, the sensor performs well in terms of comparison to the sensor's performance (PGD). However, the sensor performs well in the calculation of FAS, capturing amplitude and frequency distribution. In Figure 35 Story wise FFT plot the two waveforms are overlaid with a zoomed-in view.

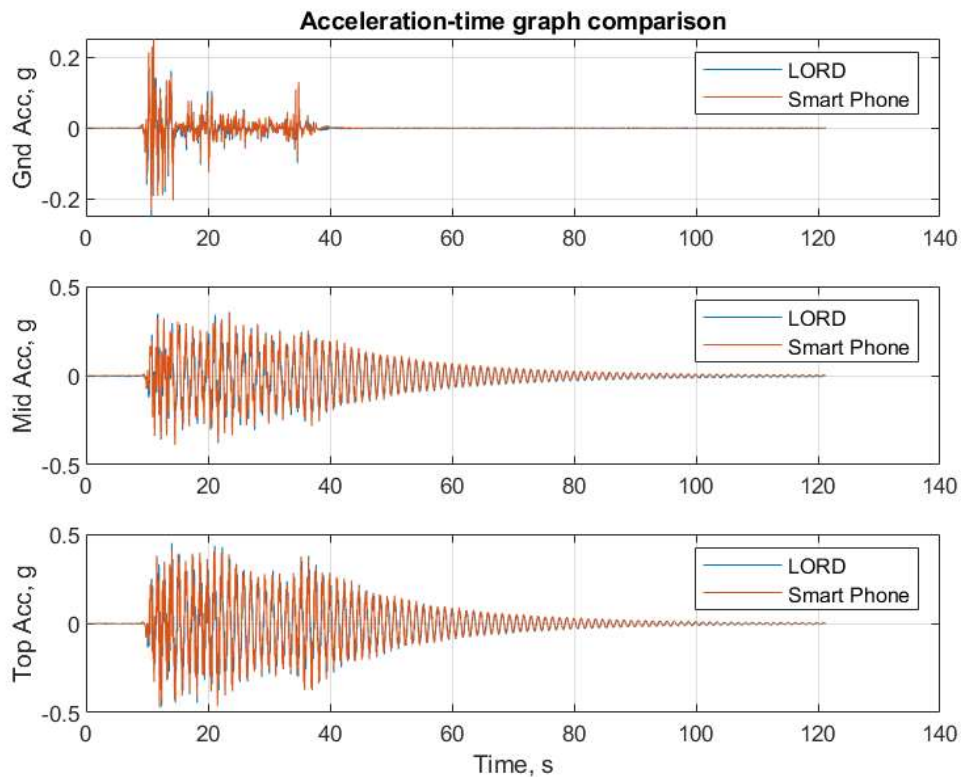


Figure 33 Story wise acceleration data

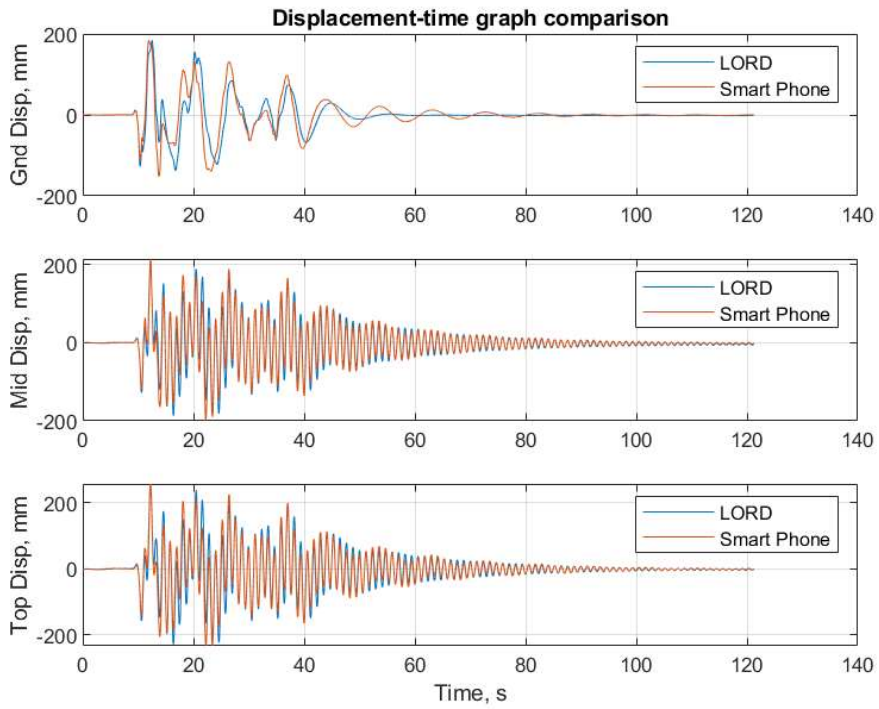
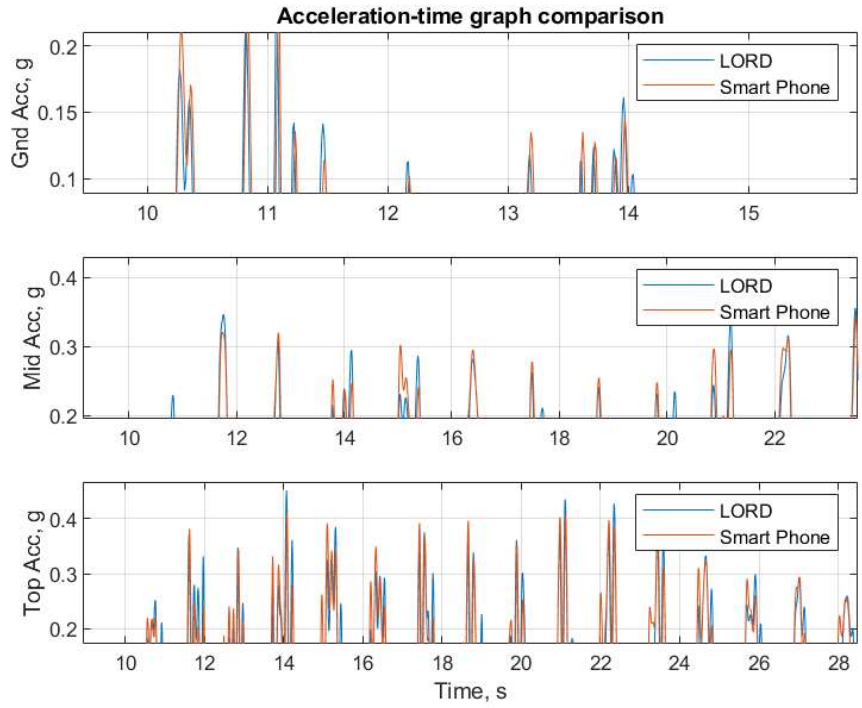
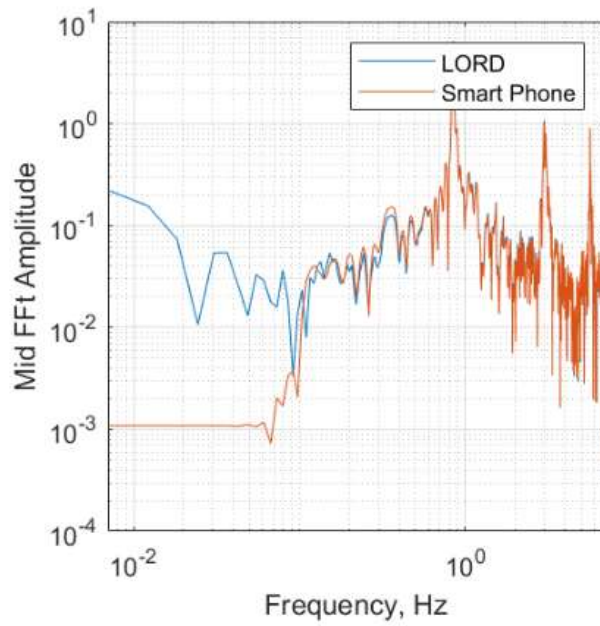
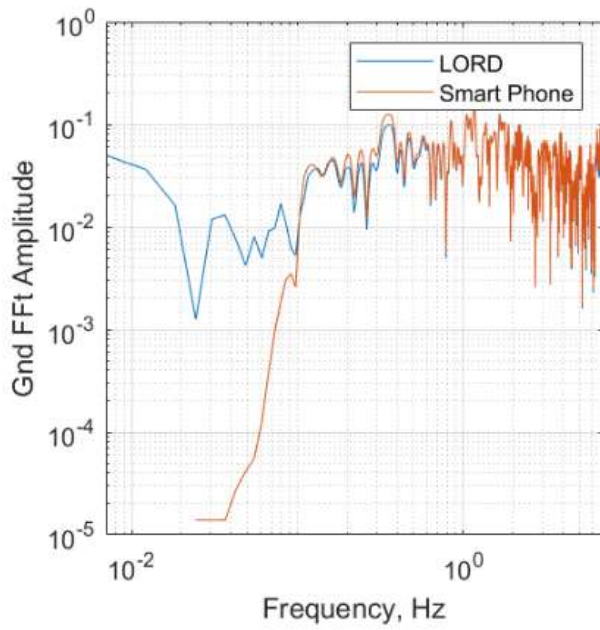


Figure 34 story wise displacement data



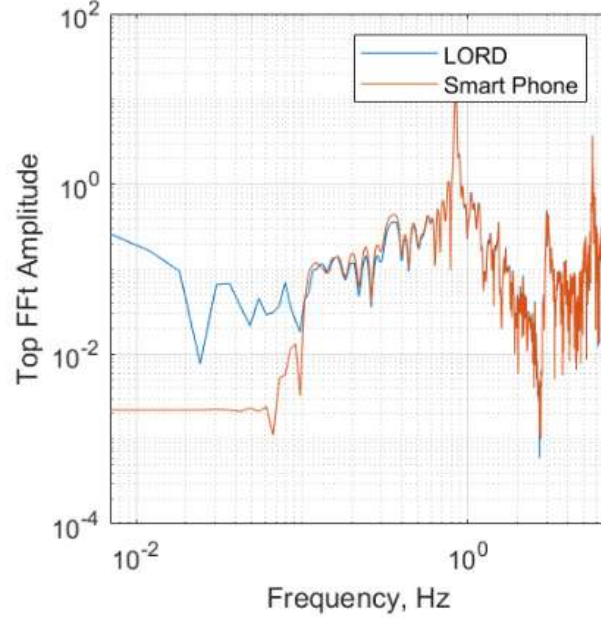


Figure 35 Story wise FFT plot

Computing ground motions measures often rely on the whole processed signal data of acceleration, hence it is important to estimate the accuracy of a acceleration data instead of just a singular peak value.. When the sensor's recorded acceleration was compared to the reference signal, a mean squared error (MSE) was calculated as follows:

$$MSE(a_{sensor}) = \frac{\sum_{i=1}^N [a_{sensor}(t_i) - a_{reference}(t_i)]^2}{N}$$

BMI-160 and LORD Accelerometer used to record the individual ground motion of a single object respectively. Samples N is the number of times the signal has been sampled. The MSE was only calculated for acceleration peaks that were larger than a 0.2-times-the-PGA amplitude cutoff, In order to prevent insignificant peaks from distorting the data (i.e. quasi motionless sensing non or strong motion).As shown in Figure 33 Story wise acceleration data, the ground motion record's PGA is shown as a function of the results. There was a wide range of MSE values, from 1.088 to 0.021 ±g2. While most of the numbers are on the low end, MSE is larger than the limit of high-fidelity sensors for seven earthquakes.



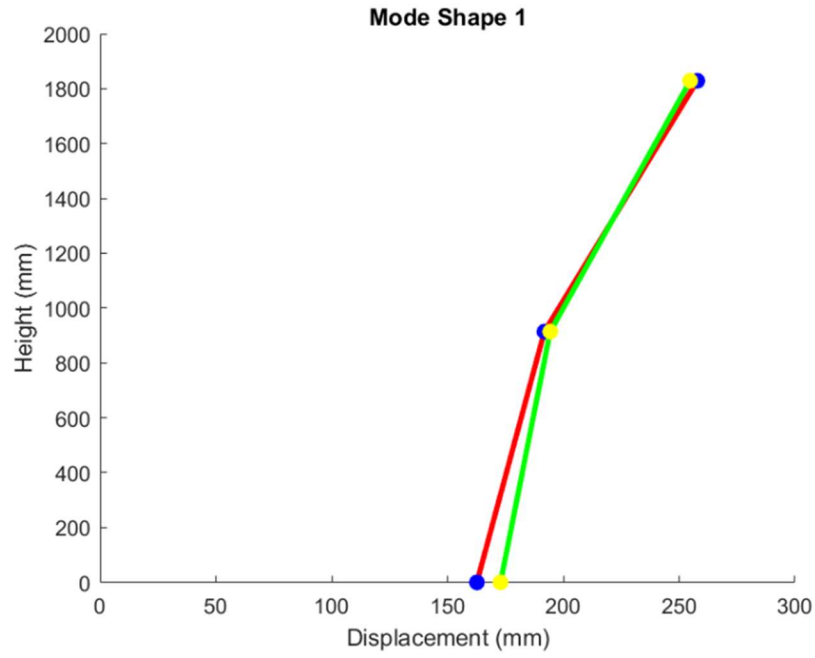


Figure 36 1st MODE Shape

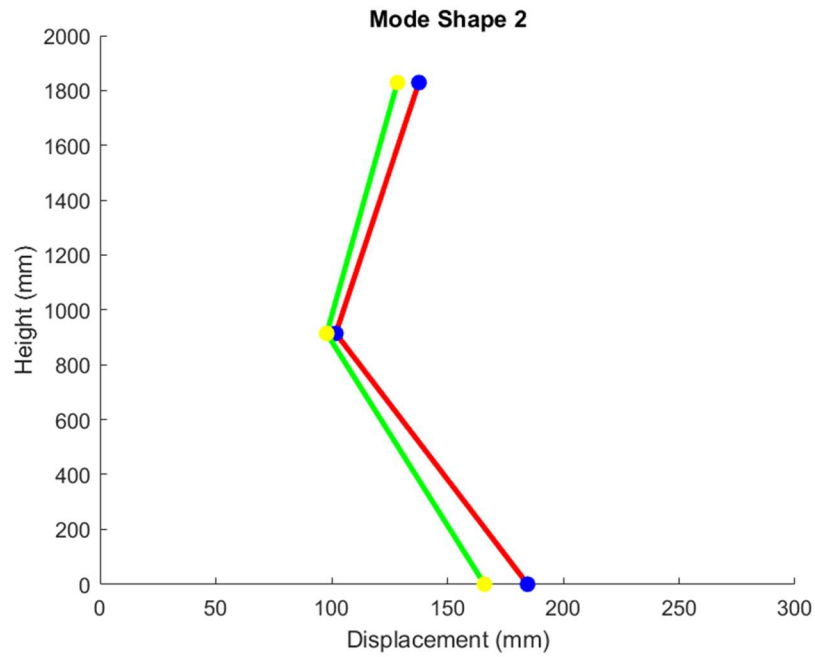


Figure 37 2nd MODE Shape

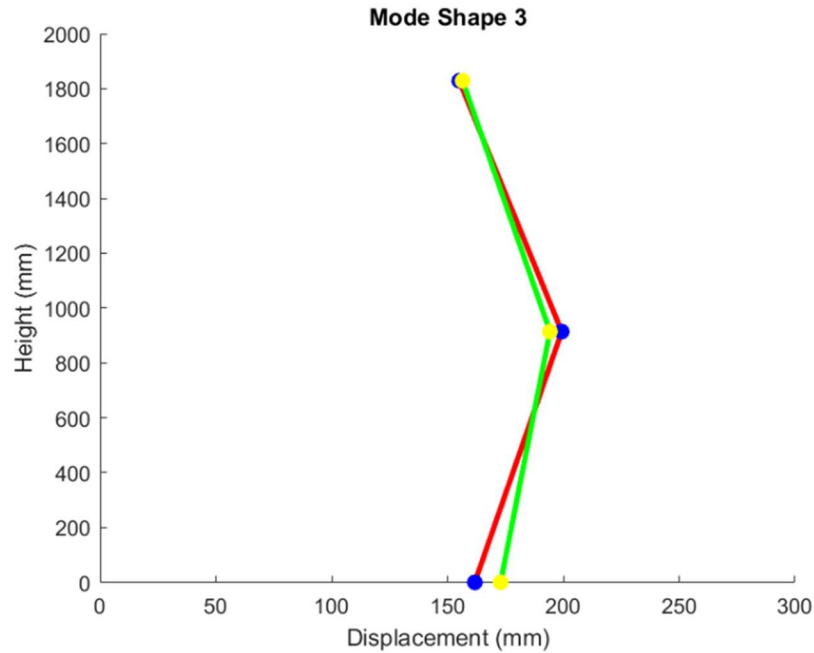


Figure 38 3rd MODE shape

#### 4.6 Four-storey frame experiment

The frame construction and properties are described in experimental program chapter. It consists of four stories and single bay. Physical properties are mentioned in Table 2 Structure Primary Parameter. The sensors were positioned in the top of the frame, same as mentioned in previous chapter MODE shape developed are shown in above mentioned figure which shows the mean error of approximately 4 %. Professional equipment was used to measure the frame's dimensions and provide a baseline for comparison. The frame was excited with an impact in the node between the stories and bars. The implementation was fast enough to keep the impact tool from diminishing. The data was saved as a text file and processed using the same algorithms as the MEMS accelerometers.

### CONCLUSIONS AND RECOMMENDATIONS

#### 5.1 Conclusion

For low-priced and accessible acceleration sensing, an open-source solution was proposed in this research and its performance was evaluated thru a series of comparison validity tests. A regularly updated open-source system should be made accessible for use in building and operating the sensor. It was built entirely from commercial electronic components.

According to the results of this investigation, the suggested sensing technique can be used as accelerometer for structural systems seismic monitoring. The sensor's MEMS analogue accelerometer has been found to have low levels of self-noise, based on standard tests. A flat amplitude transfer function was observed for the entire frequency range tested, which was constrained by the laboratory's installed capacity. However, up to the MEMS accelerometer's resonant frequency, This is a lot more than the frequency range that seismologists as well as structural earthquake engineers care about, this plain behavior is likely to be coherent. The amplitude frequency response exhibits a flat actions (such as high linearity) in the clipping tests up to a nominal maximum acceleration value 1 g, where a roll-off may be seen that is very typical. The microcontroller maintains a constant sampling rate even when running for extended periods of time. An arbitrary seismic graph tested in a linear shake table to determine the sensor's reliability under non-stationary excitations. As a whole, the sensor performed well when measuring metrics of high motion amplitudes, such as PG values of acceleration, velocity and displacement. According to the reference accelerometer's data, the full - time basis series had an MSE of 0.0036 g<sup>2</sup>. However, the sensor's underestimation of magnitudes led to less precise IA computation estimates. An average of 0.086 g has been obtained as the medium value of the quarter of the 90-percentage dependability of measurements with a confidence interval.

As a result this study's findings, a standalone genuine data gathering sensor is now within reach. This opens up a wide range of possibilities for the future. In order to improve the sensor performance, it may be necessary to test a broader variety of MEMS, particularly in the area of

absolute acceleration and noise reduction. The advancement of communication protocols and connectivity power supply options, and general sensor maintenance procedures will be the focus of future efforts.

## REFERENCES

1. Bettinali. (1990). *The dynamic analysis of large structures as a method for structural investigation*. ENEL/CRIS report 4002fb.
2. Boore, D. M. (2005). On pads and filters: Processing strong-motion data. *Bulletin of the Seismological Society of America*, 95(2), 745–750. <https://doi.org/10.1785/0120040160>
3. Boore, D. M., & Bommer, J. J. (2005). Processing of strong-motion accelerograms: needs, options and consequences. *Soil Dynamics and Earthquake Engineering*, 25(2), 93–115. <https://doi.org/10.1016/J.SOILDYN.2004.10.007>
4. Bravo-Haro, M. A., & Elghazouli, A. Y. (2018). Permanent seismic drifts in steel moment frames. *Journal of Constructional Steel Research*, 148, 589–610. <https://doi.org/10.1016/J.JCSR.2018.06.006>
5. Bremer, K., Wollweber, M., Weigand, F., Rahlves, M., Kuhne, M., Helbig, R., & Roth, B. (2016). Fibre Optic Sensors for the Structural Health Monitoring of Building Structures. *Procedia Technology*, 26, 524–529. <https://doi.org/10.1016/J.PROTCY.2016.08.065>
6. Brooks, B. ~A. (2016). Smartphone-Based Earthquake and Tsunami Early Warning in Chile. *AGU Fall Meeting Abstracts, 2016*, G31A-1045.
7. Brownjohn, J. M. W. (2007). Structural health monitoring of civil infrastructure. *Philosophical Transactions of the Royal Society A: Mathematical, Physical and Engineering Sciences*, 365(1851), 589–622. <https://doi.org/10.1098/RSTA.2006.1925>
8. Chang, F.-K. (2000, October 1). A Summary Report of The 2nd Workshop on Structural Health Monitoring, Held at Stanford University on September 8-10, 1999. Retrieved July 7, 2022, from <https://apps.dtic.mil/sti/citations/ADA384380>
9. Christensen, B. C., & Blanco Chia, J. F. (2017). *Raspberry shake-a world-wide citizen seismograph network*. In *AGU Fall Meeting Abstracts (Vol. 2017, pp. S11A-0560)*.
10. Clayton, R. W., Heaton, T., Chandy, M., Krause, A., Kohler, M., Bunn, J., ... Aivazis, M. (2012). Community Seismic Network. *Annals of Geophysics*, 54(6), 738–747. <https://doi.org/10.4401/ag-5269>
11. Clinton, J. F., & Heaton, T. H. (2002). Potential Advantages of a Strong-motion Velocity Meter over a Strong-motion Accelerometer. *Seismological Research Letters*, 73(3), 332–342. <https://doi.org/10.1785/GSSRL.73.3.332>
12. Cochran, E. S. (2018). To catch a quake. *Nature Communications*, 9(1). <https://doi.org/10.1038/s41467-018-04790-9>
13. Comerford. (1992). *The role of AI technology in the management of dam safety: the DAMSAFE system*. *Dam Eng*.
14. D'Alessandro, A. (2016). *Tiny accelerometers create Europe's first urban seismic network*. *Eos*, 97(10.1029).
15. D'Alessandro, A., Vitale, G., Scudero, S., D'Anna, R., Costanza, A., Fagiolini, A., & Greco, L. (2017). Characterization of MEMS accelerometer self-noise by means of PSD and Allan Variance analysis. *Proceedings - 2017 7th International Workshop on Advances in Sensors and Interfaces, IWASI 2017*, 159–164. <https://doi.org/10.1109/IWASI.2017.7974238>

16. DETR. (2001). *List of Panel Engineers: Reservoirs Act 1975. Department of the Environment, Transportation and the Regions.*
17. Evans, J. R., Allen, R. M., Chung, A. I., Cochran, E. S., Guy, R., Hellweg, M., & Lawrence, J. F. (2014a). Performance of Several Low-Cost Accelerometers. *Seismological Research Letters*, 85(1), 147–158. <https://doi.org/10.1785/0220130091>
18. Evans, J. R., Allen, R. M., Chung, A. I., Cochran, E. S., Guy, R., Hellweg, M., & Lawrence, J. F. (2014b). Performance of Several Low-Cost Accelerometers. *Seismological Research Letters*, 85(1), 147–158. <https://doi.org/10.1785/0220130091>
19. Fanelli. (1992). *The role of AI technology in the management of dam safety: the DAMSAFE system. Dam Eng. 3, 215–226.*
20. Fanelli, M. A. (1993). Structural Health Monitoring of Civil Infrastructure on JSTOR. Retrieved July 8, 2022, from <https://www.jstor.org/stable/25190455>
21. Horiuchi, S., Horiuchi, Y., Yamamoto, S., Nakamura, H., Wu, C., Rydelek, P. A., & Kachi, M. (2009). Home seismometer for earthquake early warning. *Geophysical Research Letters*, 36(5), 1–5. <https://doi.org/10.1029/2008GL036572>
22. Hudson. (1997). *Dynamic tests on full-scale structures In Proc. ASCE EMD Specialty Conf., UCLA, pp. 1–39.*
23. ICOLD. (2002). *No Title Automated dam monitoring systems. Guidelines and case histories. Bulletin 118. Paris: CIGB ICOLD.*
24. Jeary. (2001). *Wholistic structural appraisal. Proc. 8th Int. Conf. and Structural Safety and Reliability: ICOSSAR 200.*
25. Karakostas Christos Z, Papanikolaou Vassilis K, T. N. P. (2018). *An ultradense strong-motion urban network based on in-house designed mems accelerographs: the case of Lefkada city, Greece. In: 16th European conference on earthquake engineering.*
26. Lynch. (2005). *Monitoring the behaviour of a major box-girder bridge. In Structural assessment based on full and large-scale testing (ed. B. R. E. Garston), pp. 212–219. Watford, UK: Butterworths.*
27. M. & Schevitz, D. W. D. (1996). *Damage identification and health Characteristics:, monitoring of structural and mechanical systems from changes in their vibration UC-900., a review. Los Alamos National Labs Report LA-13070-MS1996 Damage identification and health Characteristics:, monito. UC-900., a.*
28. M, K. R. (1981). *West Sole WE Platform: Detection of damage by structural response measurements. In Proc. OTC 12 vol. 4, pp. 111-118, Houston Texas.*
29. Macrae, G. A., & Kawashima, K. (1997). Post-earthquake residual displacements of bilinear oscillators. *Earthquake Engineering and Structural Dynamics*, 26(7), 701–716. [https://doi.org/10.1002/\(SICI\)1096-9845\(199707\)26:7<701::AID-EQE671>3.0.CO;2-I](https://doi.org/10.1002/(SICI)1096-9845(199707)26:7<701::AID-EQE671>3.0.CO;2-I)
30. Maeck, J., Peeters, B., & de Roeck, G. (2001). Damage identification on the Z24 bridge using vibration monitoring. *Smart Materials and Structures*, 10(3), 512. <https://doi.org/10.1088/0964-1726/10/3/313>

31. Okundi. (2003). *Structural health monitoring of underground railways*. In *Proc. SHMII-1, structural health monitoring and intelligent infrastructures, vol. 2* (ed. Z. Wu & M. Abe), pp. 1039–1046.
32. Proulx, D. &. (n.d.). *Continuous ambient-vibration monitoring of the arch dam of Mauvoisin*. *Earthquake Eng. Struct. Dyn.* 31, 475–480.
33. Resende, M. M., Gambare, E. B., Silva, L. A., Cordeiro, Y. de S., Almeida, E., & Salvador, R. P. (2022). Infrared thermal imaging to inspect pathologies on façades of historical buildings: A case study on the Municipal Market of São Paulo, Brazil. *Case Studies in Construction Materials*, 16, e01122. <https://doi.org/10.1016/J.CSCM.2022.E01122>
34. Roberts, W. S. (2003). *Protecting heritage structures from explosive blasts*. In *Proc. Concrete in the Third Millennium, Biennial Conference of the Concrete Institute of Australia*.
35. Rodgers, P. W. (1992). Frequency limits for seismometers as determined from signal-to-noise ratios. Part 1. The electromagnetic seismometer. *Bulletin of the Seismological Society of America*, 82(2), 1071–1098. <https://doi.org/10.1785/BSSA0820021071>
36. Ross. (1995). In-Service Structural Monitoring. A State Of The Art Review. Retrieved July 7, 2022, from <https://trid.trb.org/view/415427>
37. Salvaneschi. (1996). *Applying AI to structural safety monitoring and evaluation*. *IEEE Expert Int. Syst. Appl.* 11, 24–34.
38. Severn. (1981). *Forced vibration tests and theoretical studies on dams*. In *Proc. Inst. Civil Eng.*, pp. 575–595, pt. 2 71.
39. Spidsoe, N., Berg, S., Hoen, C. & Beck, G. (1980). *Measured behaviour of platforms on the Norwegian continental shelf*. In *Proc. European Offshore Petroleum Conference and Exhibition, London*, pp. 375–391.
40. Veritas, D. N. (1977). *Rules for the design, construction and inspection of offshore structures*. Norway: DNV.
41. Welch, P. D. (1967). The Use of Fast Fourier Transform for the Estimation of Power Spectra: A Method Based on Time Averaging Over Short, Modified Periodograms. *IEEE Transactions on Audio and Electroacoustics*, 15(2), 70–73. <https://doi.org/10.1109/TAU.1967.1161901>
42. Wu & Su. (2003). *Structural health monitoring of underground railways*. In *Proc. SHMII-1, structural health monitoring and intelligent infrastructures, vol. 2*.
43. Wu, Y. M. (2014). Progress on Development of an Earthquake Early Warning System Using Low-Cost Sensors. *Pure and Applied Geophysics* 2014 172:9, 172(9), 2343–2351. <https://doi.org/10.1007/S00024-014-0933-5>
44. Yang. (1981). *Damping of an offshore platform by 'random dec' method*. In *Proc. ASCE EMD Specialty Conference—Dynamic Response of Structures, Atlanta, Georgia*, pp. 819–832.

45. Zhou, G. D., & Yi, T. H. (2013). Recent developments on wireless sensor networks technology for bridge health monitoring. *Mathematical Problems in Engineering*, 2013. <https://doi.org/10.1155/2013/947867>